DE LA RECHERCHE À L'INDUSTRIE

Modeling the rf wave at the Lower Hybrid frequency in toroidal magnetized plasmas

A major numerical challenge for current drive in tokamaks

Y. Peysson
CEA, IRFM, F-13108, Saint-Paul-lez-Durance, France

Special thanks to Dr. J. Decker

yves.peysson@cea.fr

Outline

- The current drive problem in tokamaks
- The Low Hybrid radio-frequency wave in slab geometry
- Modeling the Lower Hybrid current drive in toroidal geometry
- From ray tracing to full-wave calculations
- Conclusion and prospects

The current drive problem in tokamaks

The plasma current: a key parameter for tokamak operation

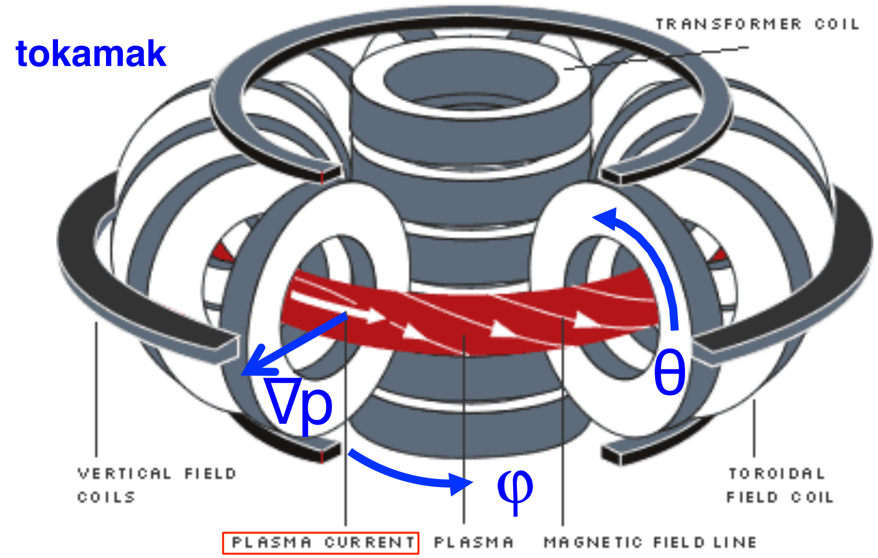

Toroidal MHD equilibrium

$$\boxed{j_{plasma}} \times B = \nabla p$$

Energy confinement

$$\tau_E \propto \boxed{I_{plasma}}/\sqrt{\boxed{P_{ext.}}}$$

Key role for stability and performances → *winding of the magnetic field lines*

$$d\varphi/d\theta \propto \int \boxed{j_{plasma}} dS$$

Control by an external source of current: $\eta = \boxed{j_{ext.}}/\boxed{P_{ext.}}$

CD efficiency

Continuous operation

Steady-state operation → the self-organized tokamak

$$j_{plasma} = \boxed{j_{configuration}} + \boxed{j_{ext.}}$$

$$\propto \nabla p$$

Self-generated (bootstrap) $\nabla \cdot j_{\perp} \neq 0 \longrightarrow j_{||} \neq 0$

forced

The current drive efficiency is too low for achieving $j_{plasma} \approx j_{ext.}$ with $P_{ext.} << P_{fusion}$

P. -H. Rebut et al., Plasma Phys. Control. Fusion, 35 (1993) A3-A14

J. Decker, Y. Peysson, et al., Nucl. Fusion, 51 (2011) 073025

$P_{\text{Lower Hybrid}}$ = 20 MW → I_{LH} = 0.6-1.0 MA (ITER)

Self-organized (advanced tokamak) scenarios

Steep *pressure gradient ∇p*
+
low plasma current I_p

$I_{\text{self-generated}}/I_p$ ≥ 60% (Iter)

$$\tau_E \propto \boxed{H} \times I_p/\sqrt{P_{ext.}}$$

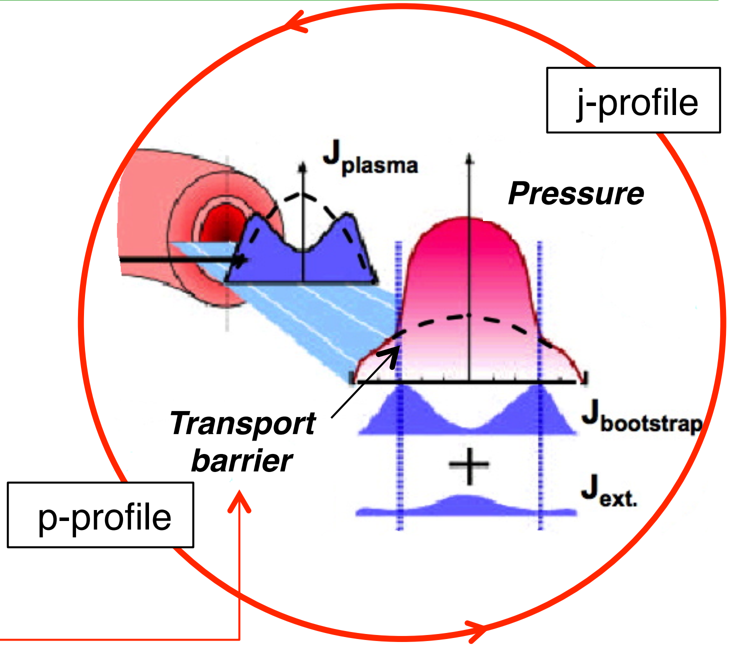

Keywords to characterize an appropriate method for driving a current in tokamaks

- **Steady-state** → *for continuous operation*
- **Localization** → *capability to drive a current from the core to the edge of the plasma with broad or narrow profiles.*
- **Controlability** → *for real-time modification of the current level and spatial localization from parameters at launch*
- **Efficiency** → *the smallest possible fraction of fusion power is used for driving a current in the plasma*

rf waves provide a set of very powerful tools for current drive

From pulsed to steady-state operation beyond the transformer

0-D

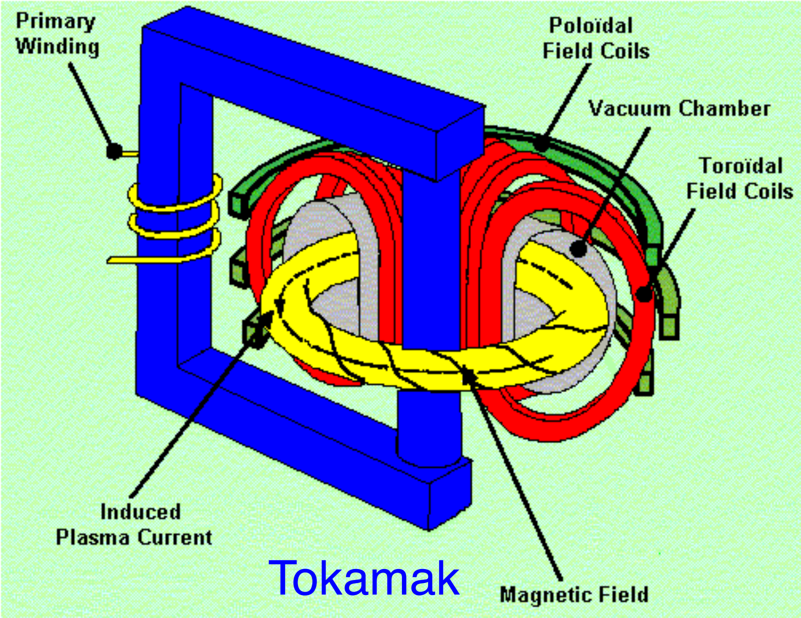

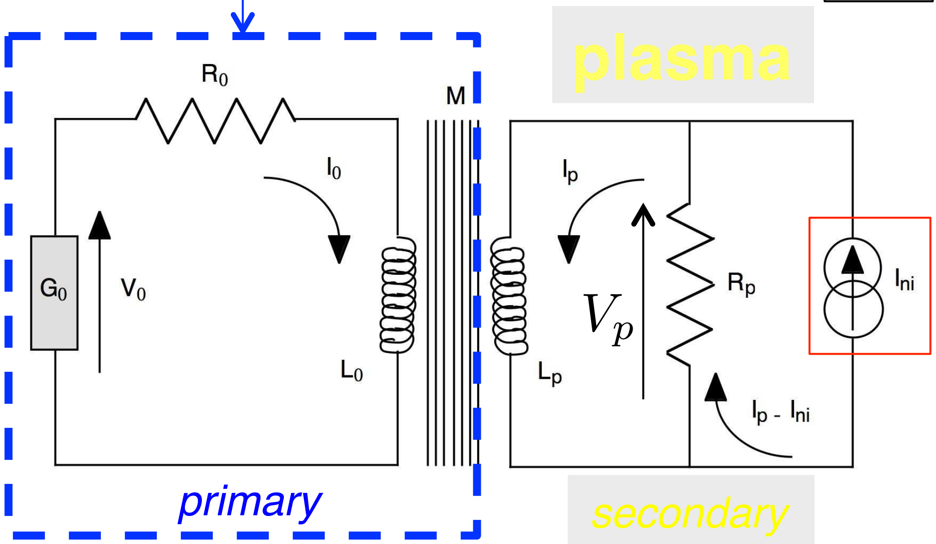

The plasma duration is limited by the consumption of the magnetic flux Φ_M

$$M\frac{dI_p}{dt} + L_0\frac{dI_0}{dt} + R_0 I_0 = V_0$$

$$M\frac{dI_0}{dt} + L_p\frac{dI_p}{dt} + \underbrace{R_p\left(I_p - I_{ni}\right)}_{V_p} = 0$$

Heating $\quad \sim T_e^{-3/2}$ $\quad$ Inductive current

$$\frac{d\Phi_M}{dt} = L_0\frac{dI_0}{dt} = -\boxed{R_p}\frac{L_0}{M}\left(I_p - \boxed{I_{ni}}\right)$$

Non-inductive source of current

F. Kazarian et al., Plasma Phys. Control. Fusion ***38*** *(1996) 2113–2131*

Convergence towards stationnary regime with a non-inductive source of current

Constant Φ_M feedback control → single time scale $\tau_T^{fast} \simeq 1.3s$

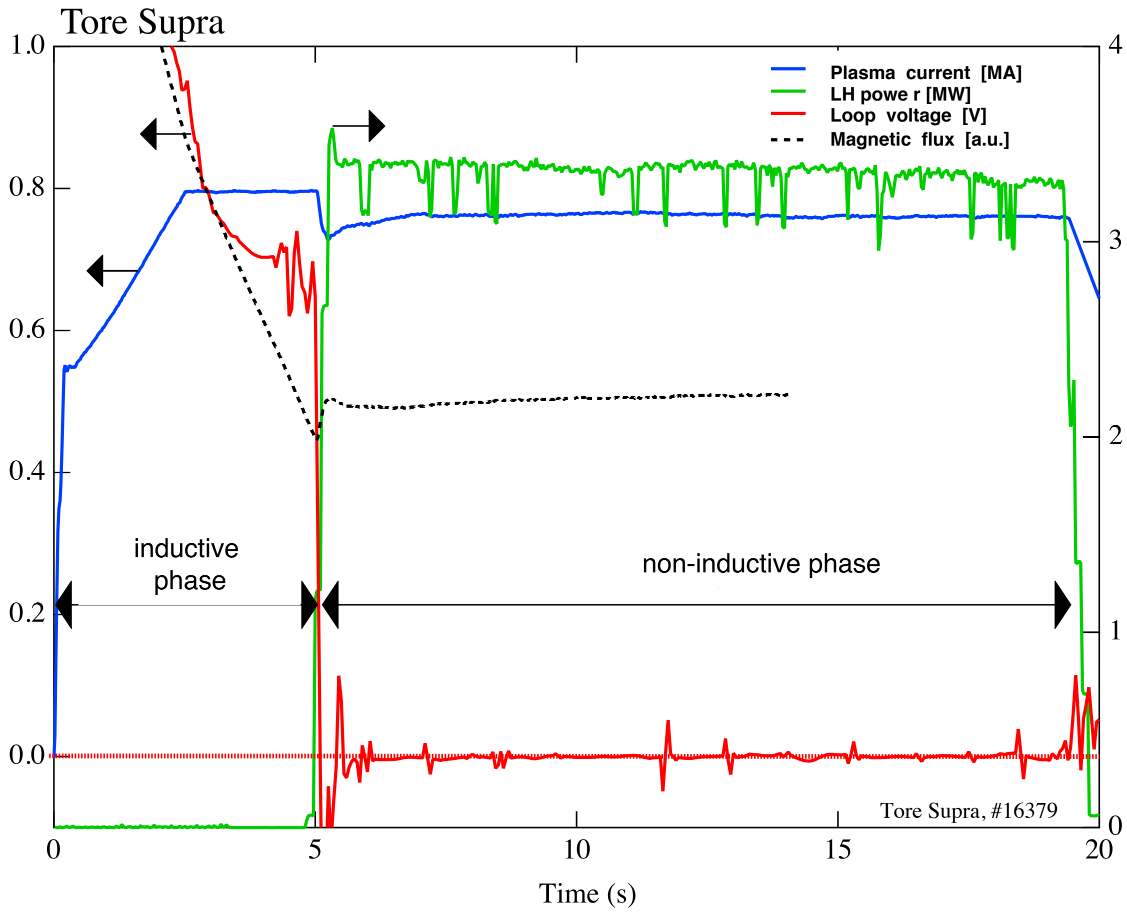

$V_p = 0V$

Reproducible stationnary regime, I_p level adjusted with $P_{LH} \rightarrow \eta$

From a stationnary to a steady-state regime: current resistive diffusion

1-D

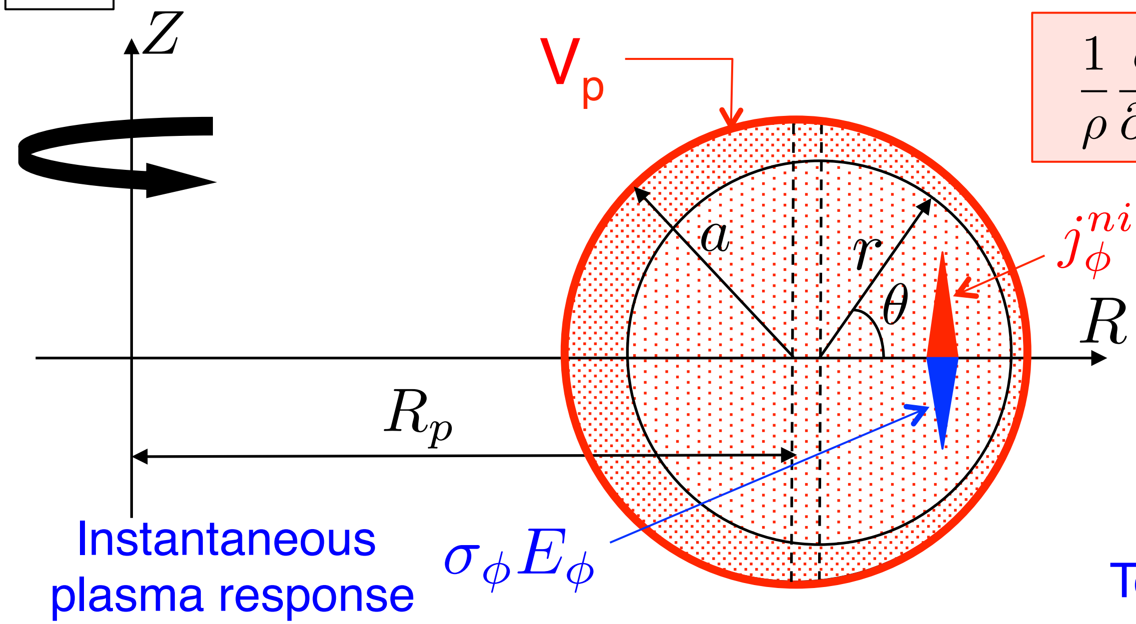

Ampère's + Faraday's + Ohm's law

$$\boxed{\frac{1}{\rho}\frac{\partial}{\partial\rho}\left(\rho\frac{\partial E_\phi}{\partial\rho}\right) = \frac{\partial}{\partial\tau}\underbrace{\left(E_\phi + j_\phi^{ni}/\sigma_\phi\right)}_{j_\phi}}$$

Resistive time: $\tau_r = \mu_0\sigma_\phi a^2$

Fundamental eigenmode:

$$\tau_r^* = \tau_r/\lambda_1^2 \qquad J_1(\lambda_1) = 0$$

Tore Supra (a = 0.7m) @ T_e = 5 keV

$$\boxed{\tau_r \simeq 16.8s}$$

The current density profile evolves on a very long time scale at high temperature → **current profile preshaping when the plasma is cold**

Stationnary regime: $dI_p/dt = 0$

Steady-state regime: $dj_\phi/dt = 0 \longrightarrow E_\phi = 0$ everywhere

Convergence towards steady-state regime with a non-inductive source of current

Steady-state operation: $t \gg \tau_r^* \gg \tau_{fast}$

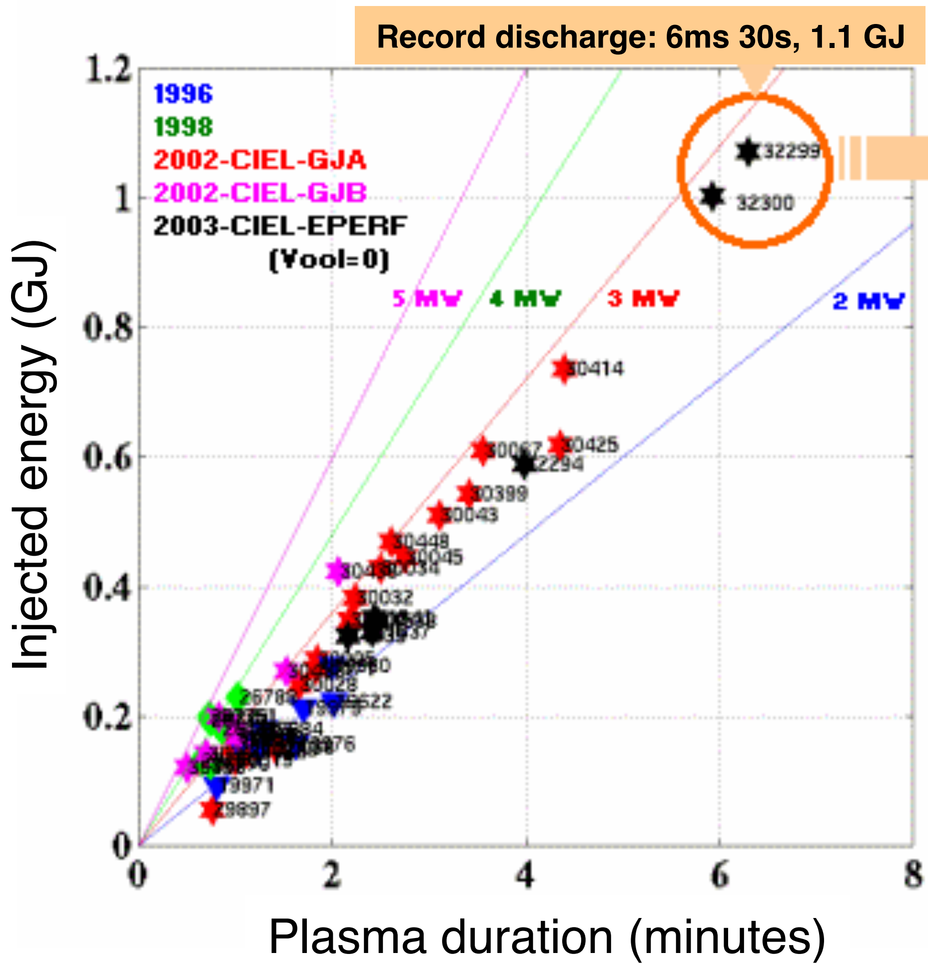

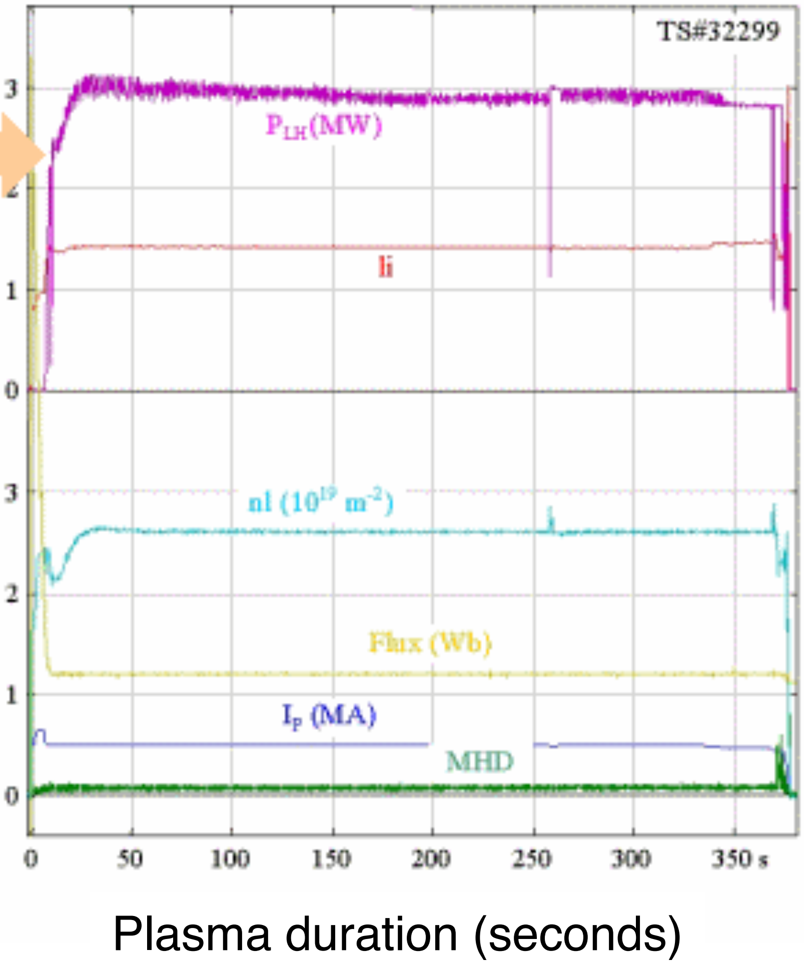

D. van Houtte et al., Fusion Engineering and Design 74 (2005) 651–658

Time scales and the physics of current sources

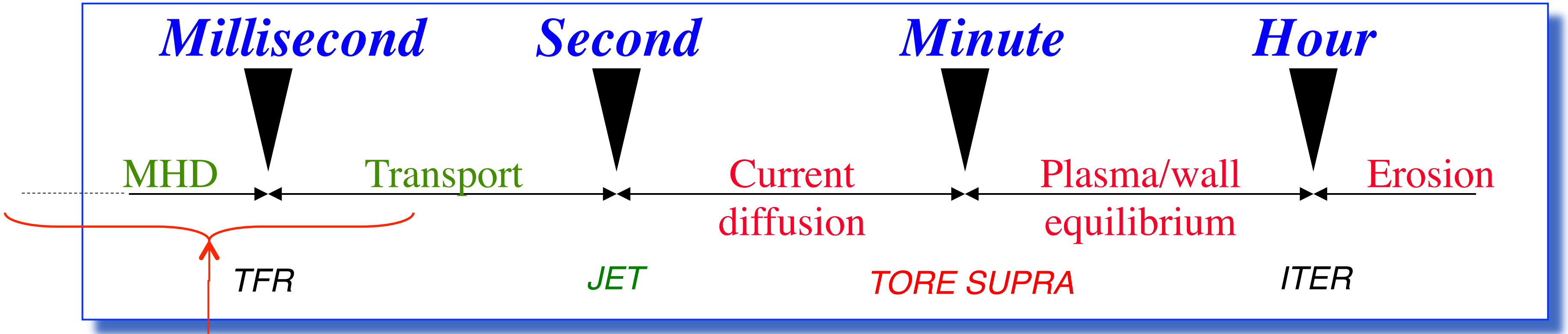

Physics of non-inductive rf current sources

$$\overbrace{\omega_{pe}^{-1} \le \omega_{ce}^{-1} \ll \omega_{pi}^{-1} \le \omega_{ci}^{-1} \ll \tau_{b,t} \ll \left(\tau_{QL}, \tau_{coll}, \tau_{E_\parallel}\right) \le \tau_{art}}^{\text{Physics of non-inductive rf current sources}} \le \overset{\text{confinement}}{\tau_{Energy}} \ll \overset{\text{transformer}}{\tau_T^{fast}} \ll \overset{\text{Current diffusion}}{\tau_r^{*}}$$

Large time scale separability makes modeling easier !

(hot plasma in large machines)

code modularity

Y. Peysson and J. Decker, Theory of fusion plasmas, 2008, 1069, AIP, 176-187

Integrated tokamak modeling and current sources (CRONOS, ITM,…)

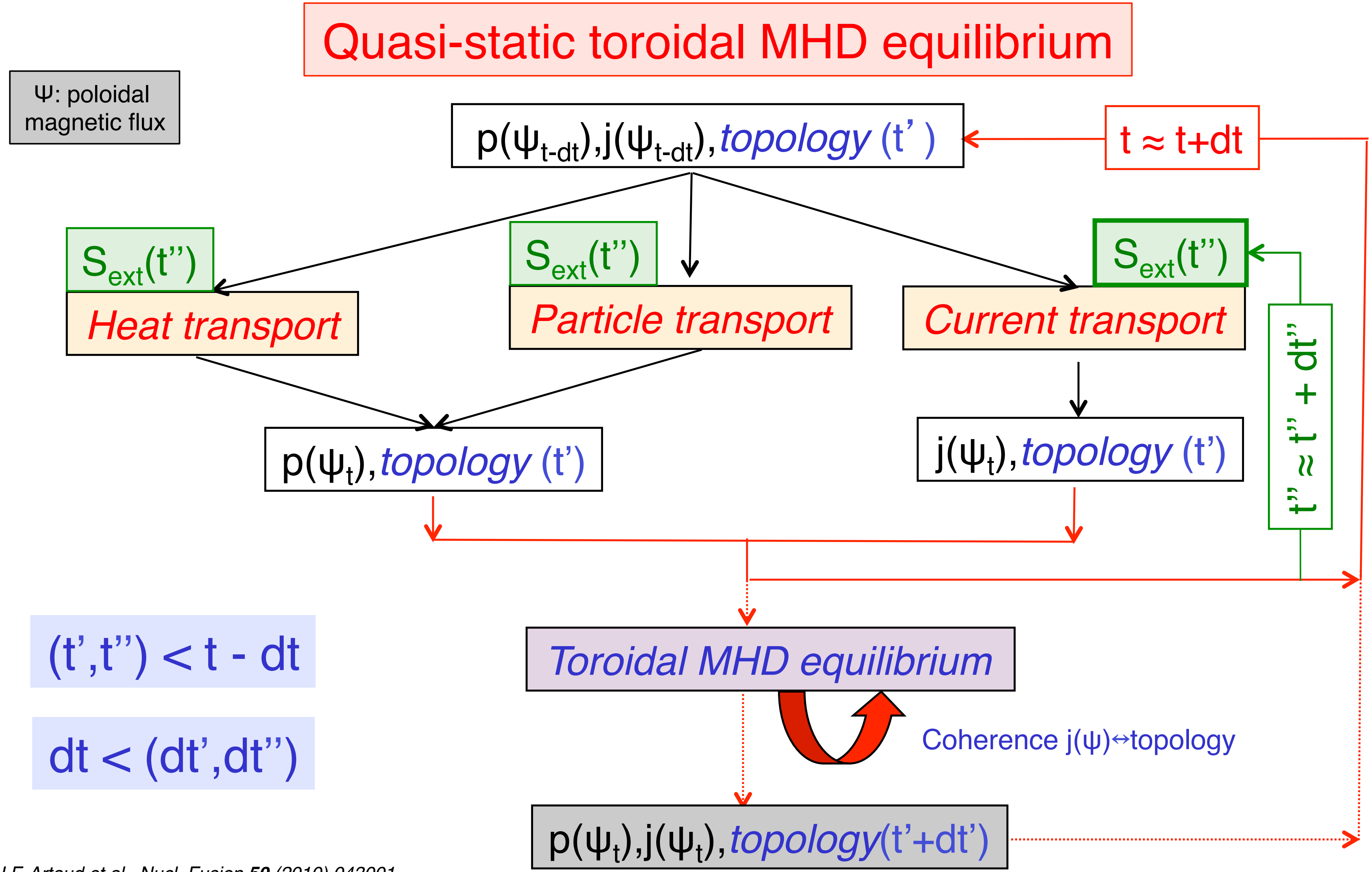

J.F. Artaud et al., Nucl. Fusion ***50*** *(2010) 043001*

Numerical issues of current drive modeling

- **High-modularity** → *for code maintenance/evolution and interoperability (physics is the limitation).*
- **Fast calculation** → *each module is part of a chain of codes in which it may be called thousands of times : fast algorithms and use of parallel processing CPU/GPU.*
- **Reduced memory consumption** → *Flexible adaptative grids for refined calculations with an appropriate metric.*
- **Robust algorithms** → *Define physical/numerical operational limits to avoid failure of the whole chain of calculations*
- **Hardware/software** → *top level (physics) programmation almost independent of the hardware (heterogenous clusters)*

The Lower Hybrid wave in slab geometry

Current drive efficiency: direct parallel push

$$\frac{\Delta J}{\Delta P} = \frac{q_e}{m_e v_\parallel \nu_{coll}(v_\parallel)}$$

$$\nu_{coll}(v_\parallel \gg v_{te}) \propto \frac{n}{v_\parallel^3}$$

$$\boxed{\frac{\Delta J}{\Delta P}(v_\parallel \gg v_{te}) \simeq \frac{q_e}{m_e}\frac{v_\parallel^2}{n}}$$

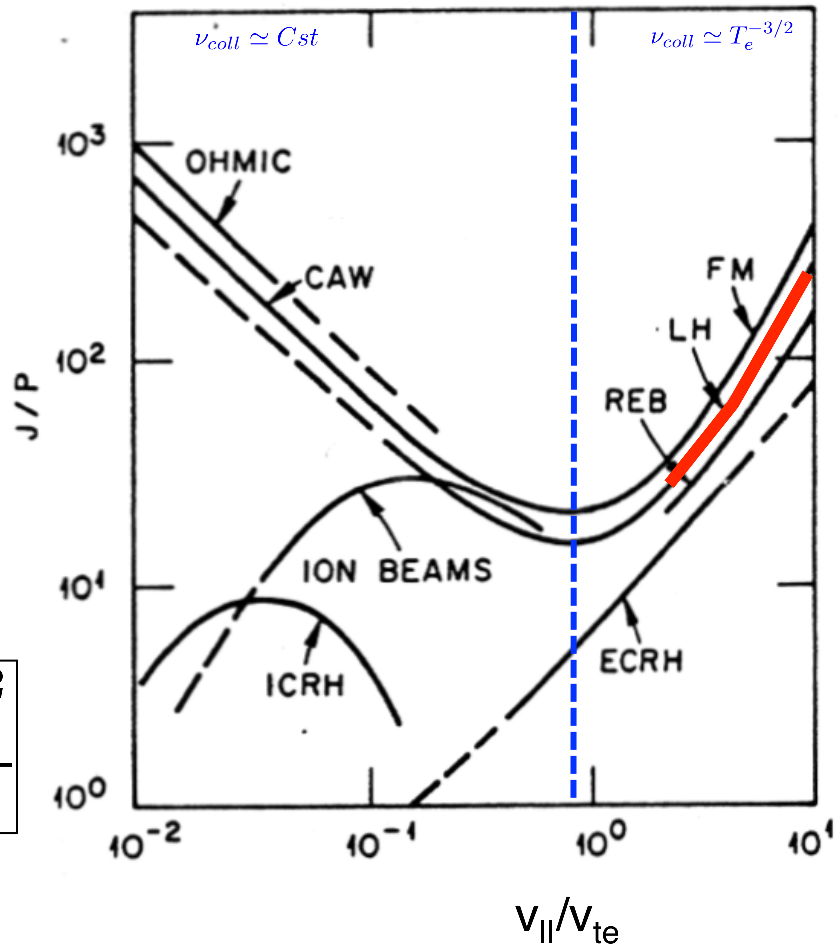

N.J. Fisch, Rev. Mod. Phys., 1987, 59, 1, pp. 175-234

Resonnant electron acceleration process

Longitudinal kinetic resonance (Landau) : $\mathbf{v}_{\parallel} = \dfrac{\mathbf{c}}{\mathbf{n}_{\parallel}}$

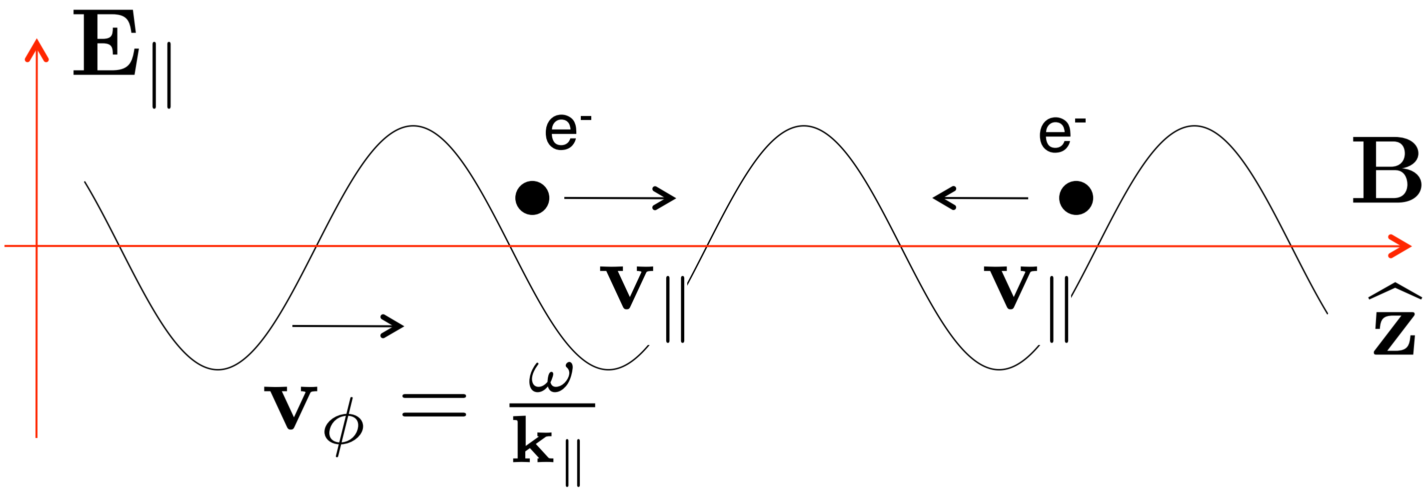

$\mathbf{v}_{\parallel} < \mathbf{v}_{\phi}$ are accelerated

$\mathbf{v}_{\parallel} > \mathbf{v}_{\phi}$ are slowed down

$\partial f/\partial v_{\parallel} < 0 \rightarrow$ more electrons gain parallel kinetic energy, irreversible momentum transfer (LH wave → electrons)

LH wave characteristics from current drive principles

For typical tokamak plasmas :

$$\mathbf{T_e = (3 - 10)\,keV}$$

$$\mathbf{v_{te}/c \simeq (0.07 - 0.14)}$$

$$\Downarrow$$

$$\boxed{\mathbf{n_{\|}\,(5 \times v_{te}) \simeq (1.4 - 3)}}$$

$$\Downarrow$$

$$\mathbf{E_{c\|}\,(5 \times v_{te}) \simeq (30 - 130)\,keV}$$

Problem: there is no electron at these energies with a Maxwellian distribution function (plasma almost transparent) !

The spectral gap problem for the LH wave

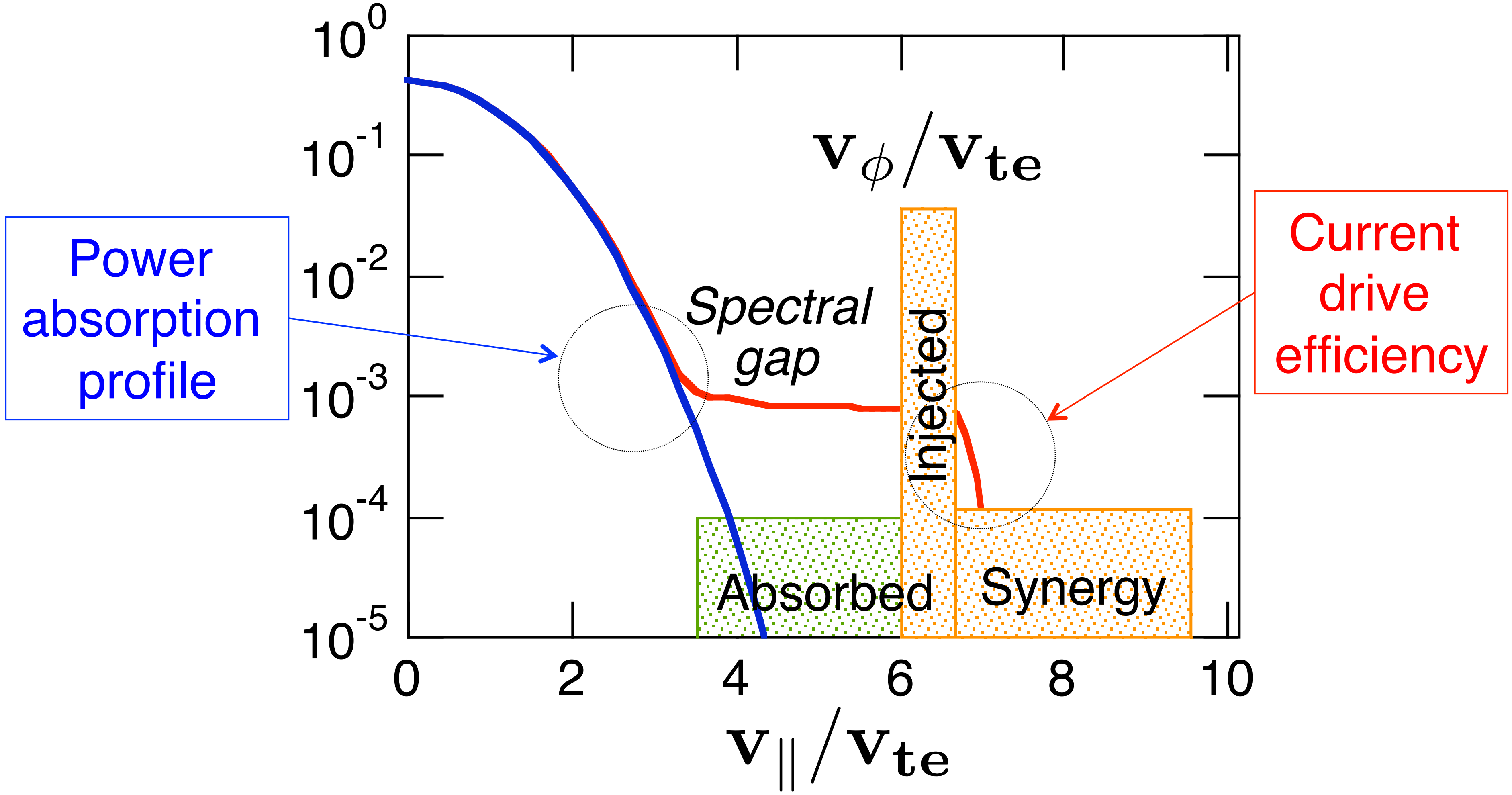

Many mechanisms may contribute to bridge the **spectral gap**

Slab geometry

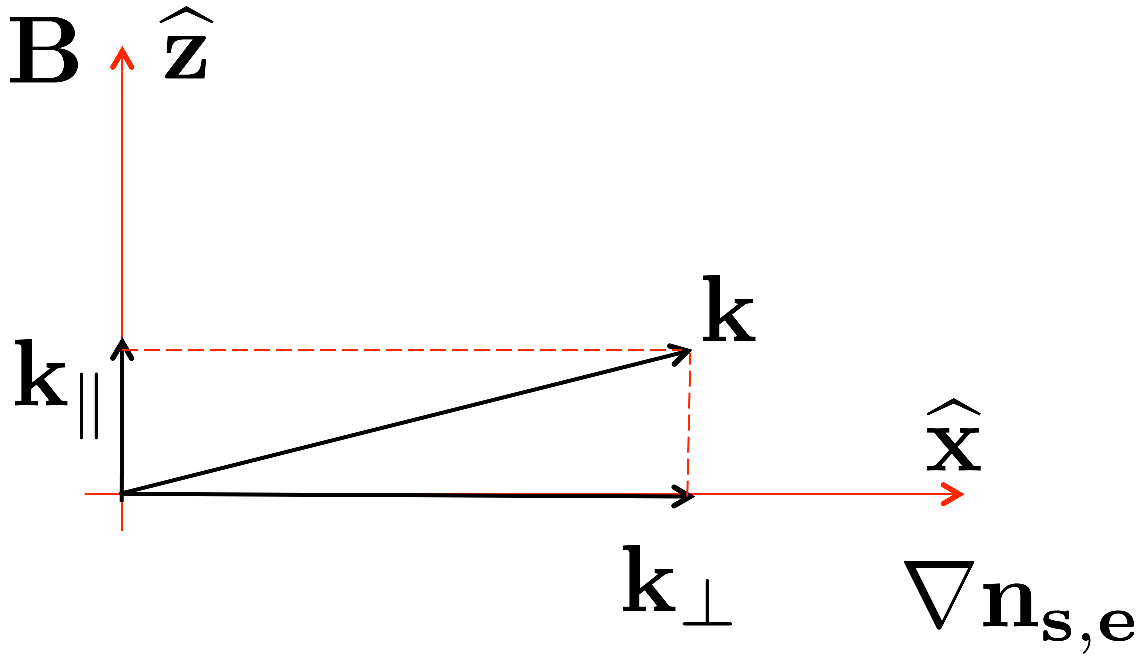

The electrostatic LH wave dispersion relation

Cold plasma approximation: $\lambda_{LH} >> L_{Debye} = v_{Te}/\omega_{pe}$

$$\boxed{\mathbf{k_{\parallel}^2}\varepsilon_{\perp} + \mathbf{k_{\perp}^2}\varepsilon_{\parallel} = \mathbf{0}}$$

Stix notation

$$\varepsilon_{\perp} \equiv \mathbf{S} = \mathbf{1} + (\omega_{\mathbf{pe}}/\mathbf{\Omega_{ce}})^{\mathbf{2}} - (\omega_{\mathbf{ps}}/\omega)^{\mathbf{2}}$$

$$\varepsilon_{\parallel} \equiv \mathbf{P} = \mathbf{1} - (\omega_{\mathbf{pe}}/\omega)^{\mathbf{2}} - (\omega_{\mathbf{ps}}/\omega)^{\mathbf{2}}$$

assuming $|\mathbf{k}| \gg |\nabla \mathbf{n}/\mathbf{n}|$ (WKB approx.)

and $\mathbf{\Omega_{cs}^2} \ll \omega^{\mathbf{2}} \ll \mathbf{\Omega_{ce}^2}$ (no cyclotron resonance)

*M. Brambilla, **Kinetic Theory of Plasma Waves**, Oxford Science Publications, 1998*

The electrostatic LH wave dispersion relation

Solving the dispersion relation for $\mathbf{k}_\perp^2$ yields

$$\boxed{\mathbf{k}_\perp^2 = -\mathbf{k}_\parallel^2 \varepsilon_\parallel / \varepsilon_\perp \quad \rightarrow \quad \mathbf{k}_\perp^2 \simeq \frac{\mathbf{m_s}}{\mathbf{m_e}} \frac{\omega_{\mathbf{LH}}^2}{\omega^2 - \omega_{\mathbf{LH}}^2} \mathbf{k}_\parallel^2}$$

→ plasma resonance for $\varepsilon_\perp = \mathbf{0}$ $\quad (\mathbf{k}_\perp \rightarrow \infty)$

→ plasma cut-off for $\varepsilon_\parallel = \mathbf{0}$ $\quad (\mathbf{k}_\perp = \mathbf{0})$

Resonance frequency : $\boxed{\frac{\mathbf{1}}{\omega_{\mathbf{LH}}^2} \equiv \frac{\mathbf{1}}{\omega^2} = \frac{\mathbf{1}}{\mathbf{\Omega_{cs} \Omega_{ce}}} + \frac{\mathbf{1}}{\omega_{\mathbf{ps}}^2}}$

Cut-off frequency : $\omega_{\mathbf{pe}} = \omega_{\mathbf{LH}} \rightarrow \mathbf{n_{cut}}$

The wave does not propagate in vacuum → **antenna**

The LH wave frequency and wavelength

For typical tokamak parameters :

$$\mathbf{B = (1 - 10)\,T}$$

$$\mathbf{n = \left(10^{18} - 10^{20}\right) m^{-3}}$$

$$\Downarrow$$

$$\mathbf{f_{LH}} = \omega_{\mathbf{LH}}/\mathbf{2}\pi = \mathbf{(0.5 - 5)\,GHz}$$

$$\lambda_{\mathbf{LH,vac}} = \mathbf{c/f_{LH} = (60 - 6)\,cm}$$

$$\varepsilon_\perp \simeq \mathbf{1} \ll \left|\varepsilon_{||}\right| \qquad \boxed{\mathbf{k_\perp^2/k_{||}^2 \gg 1}}$$

$$\Rightarrow \quad \lambda_\perp \ll \lambda_{||} \qquad \lambda_{||} = \frac{c}{fn_{||}}$$

$$\Rightarrow \quad \lambda_{||} \simeq 1cm \qquad \lambda_\perp \simeq 1mm$$

The electromagnetic LH wave dispersion relation

Two propagation modes in the LH range of frequencies

$$\left|\varepsilon_{\|}\right| \gg \varepsilon_{\perp}, \varepsilon_{\mathbf{xy}} \quad \rightarrow \quad \mathbf{P_0 > 0, P_2 < 0}$$

$$\mathbf{n_{\perp}^2 = \frac{1}{2P_4}\left(-P_2 \pm \sqrt{\Delta}\right)}$$

$$\mathbf{\Delta = P_2^2 - 4P_0P_4}$$

- Slow wave branch (+) → small $\omega/\mathbf{k}_{\perp}$
- Fast wave branch (-) → large $\omega/\mathbf{k}_{\perp}$

cold confluence

$$\mathbf{\Delta = 0}$$

P.T. Bonoli, IEEE Trans. on Plasma Sci., 1984, PS-12, 2, pp. 95-107

Stix-Golant LH wave accessibility condition

The condition $\boldsymbol{\Delta = \Delta\left(n_{\|}, n_{e,s}, B\right) > 0}$

is required for the slow wave not to mode convert along the path of propagation: **LH wave accessibility**

Stix-Golant criterion

$$\boxed{\mathbf{n_{\|} > n_{\|a} = \sqrt{S} + \frac{D}{\sqrt{-P}} \propto \frac{\sqrt{n}}{B}}}$$

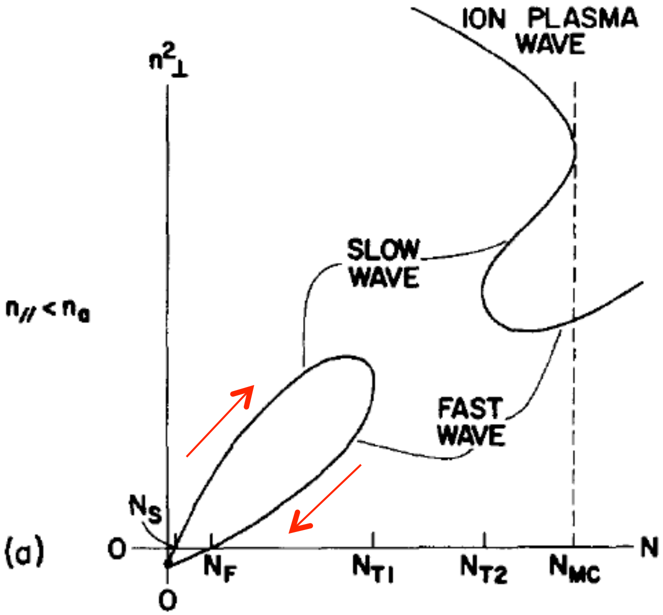

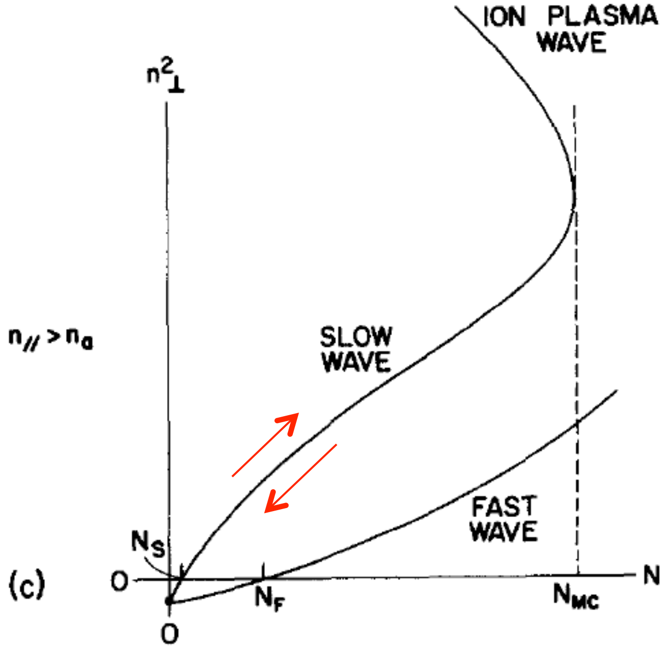

P.T. Bonoli and R.C. Englade, Phys. Fluids, 1986, 29, 9, pp. 2937-2950

Slow/fast modes

$$\left(\frac{E_x}{E_z}\right)_{slow} \simeq \frac{n_\parallel n_\perp}{n_\parallel^2 - S} \sim \sqrt{-\frac{P}{S}} \sim \sqrt{\frac{m_s}{m_e}}$$

$$\left(\frac{E_x}{E_z}\right)_{fast} \simeq \frac{P}{n_\parallel n_\perp} \sim \frac{m_s}{m_e}$$

$$\boxed{E_z \ll E_{x,y}} \qquad \boxed{\frac{E_{z,slow}}{E_{z,fast}} \sim \sqrt{\frac{m_s}{m_e}} \gg 1}$$

- With a larger parallel electric field, the slow wave more favorable for **Landau damping** $\boxed{v_e \simeq v_\Phi}$
- Fast LH wave contribution in high temperature plasmas only.
- LH wave may interact also by cyclotron resonance interaction $\rightarrow$ **α particles**

- Current drive → slow wave (electrostatic mode, large $E_{||}$, easiest mode to launch regarding the edge cut-off condition)

- $\omega \geq \omega_{LH}$ → no LH resonance (no direct ion heating).

- Thermal corrections for the slow wave branch have marginal consequences on the level of the driven current.

- **Slab geometry is valid in the vicinity of the antenna only**. *In toroidal geometry, beam/ray-tracing or full-wave calculations must be performed for describing the evolution of the poloidal mode number along the propagation path, because of the poloidal asymmetry of the magnetic equilibrium.*

Modeling the Lower Hybrid current drive in toroidal geometry

Standard rf current source module

- The ray-tracing is function of f_M.
- The wave amplitude, i.e. the quasilinear diffusion coefficient D_{ql} must be calculated self-consistently with the distribution f_0.
- <u>Global consistency</u>: *power lost by the wave = power gained by electrons from quasilinear operator*

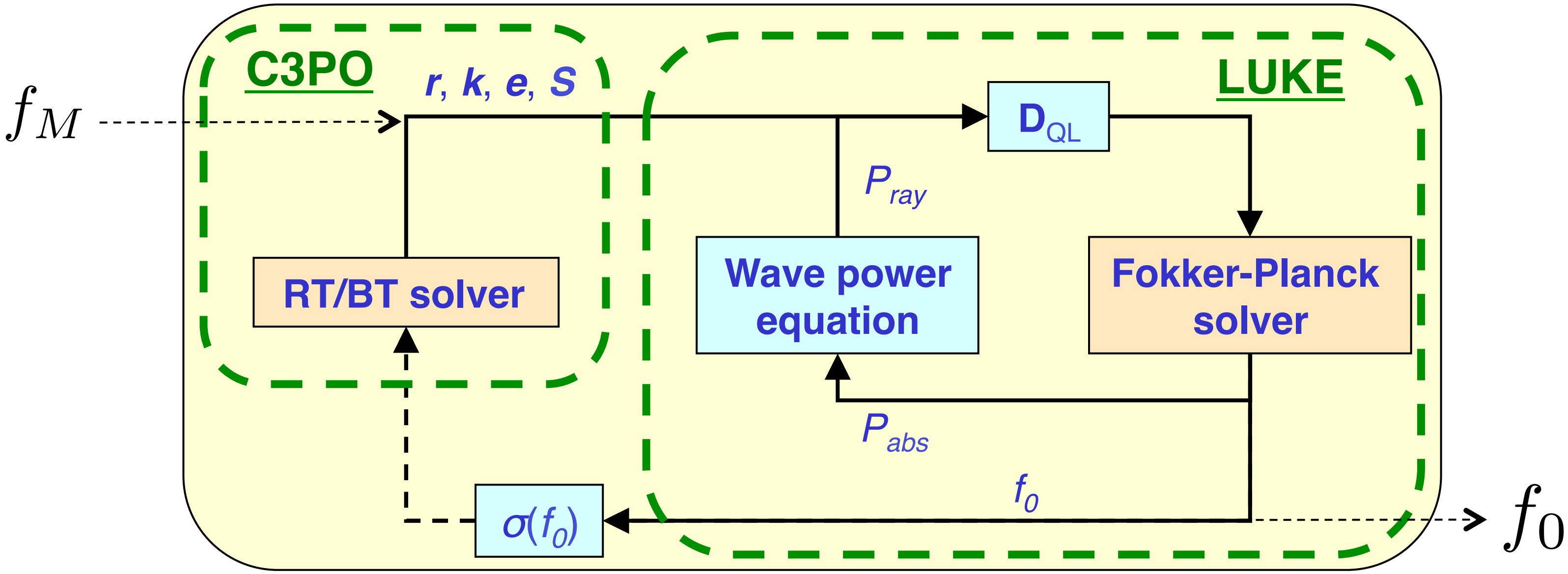

Weak damping approximation

Y. Peysson and J. Decker, Theory of fusion plasmas, 2008, 1069, AIP, 176-187

The ray tracing equations

- at all points of the ray trajectory $\mathcal{D} = \det \mathbb{D}^{\mathbf{H}}_{\mathbf{k},\omega} = \mathbf{0}$

$$\delta\mathcal{D} = \frac{\partial \mathcal{D}}{\partial \mathbf{X}} \cdot \delta\mathbf{X} + \frac{\partial \mathcal{D}}{\partial t}\delta t + \frac{\partial \mathcal{D}}{\partial \mathbf{k}} \cdot \delta\mathbf{k} + \frac{\partial \mathcal{D}}{\partial \omega}\delta\omega = 0$$

- Hamiltonian ray equations

$$\begin{cases} \dfrac{d\mathbf{X}}{dt} = -\dfrac{\partial \mathcal{D}}{\partial \mathbf{k}} \Big/ \dfrac{\partial \mathcal{D}}{\partial \omega} \\[2ex] \dfrac{d\mathbf{k}}{dt} = \dfrac{\partial \mathcal{D}}{\partial \mathbf{X}} \Big/ \dfrac{\partial \mathcal{D}}{\partial \omega} \end{cases}$$

Y. Peysson et al., 2012 Plasma Phys. Control. Fusion 54 045003

Curvilinear metric consistent with MHD equilibrium (nested magnetic flux surfaces)

$$\begin{cases} \mathbf{k} = k_R\hat{\mathbf{R}} + k_Z\hat{\mathbf{Z}} + k_\phi\hat{\phi} \\ \mathbf{k} = k_\rho \left\|\nabla\rho\right\| \widehat{\rho} + \dfrac{m}{r}\widehat{\theta} + \dfrac{n}{R}\widehat{\phi} \end{cases}$$

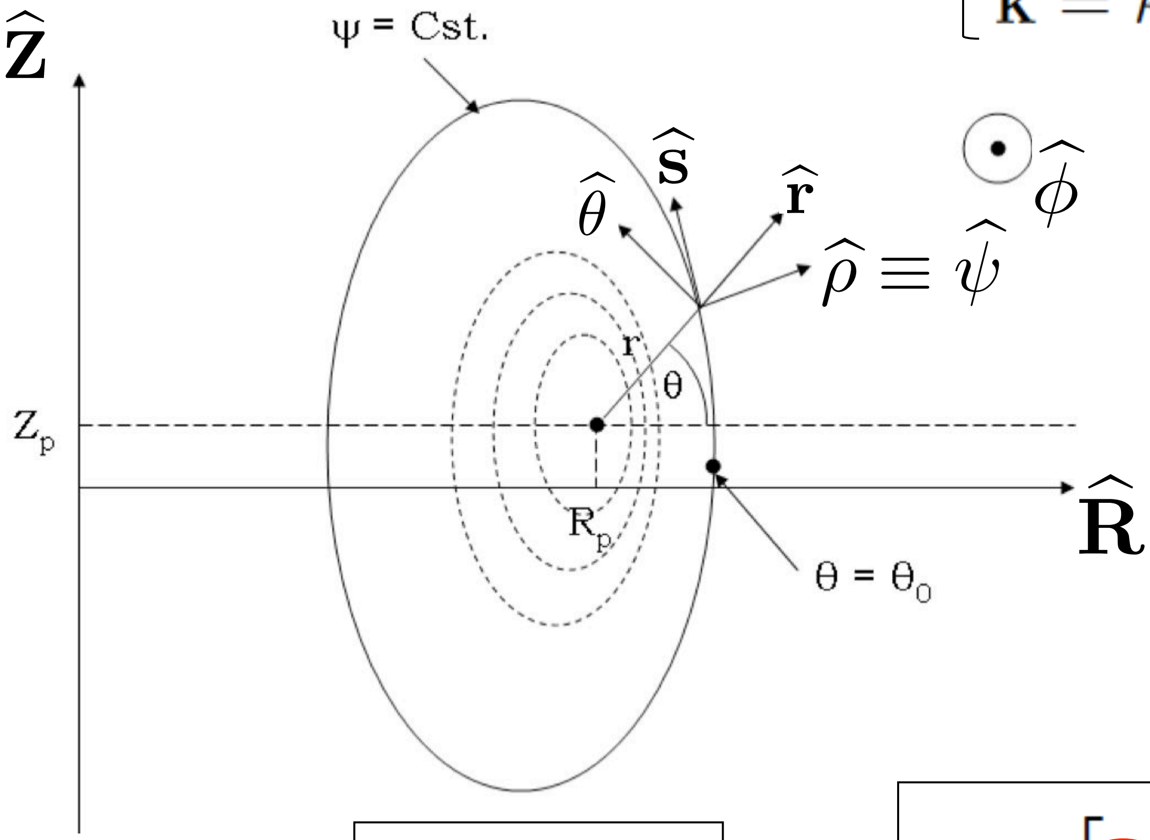

$$\boxed{\hat{\rho}\cdot\hat{\mathbf{r}} = \cos\alpha}$$

covariant coordinates

$$k_\rho = \frac{\hat{\mathbf{r}}\cdot\mathbf{k}}{\left\|\nabla\rho\right\|\cos\alpha}$$

$$m = \frac{r\hat{\mathbf{s}}\cdot\mathbf{k}}{\cos\alpha}$$

$$n = R\hat{\phi}\cdot\mathbf{k}$$

$$k_\parallel = \left[\sigma_I \cos\alpha \frac{B_P}{B}\frac{m}{r} + \sigma_B \frac{B_T}{B}\frac{n}{R}\right]$$

Y. Peysson et al., 2012 Plasma Phys. Control. Fusion 54 045003

Parallel refractive index upshift in tokamaks

- The toroidal wave number ***n*** is a constant of the ray motion (axisymmetry)

- The poloidal wave number ***m*** evolved along the raypath because of the poloidal asymmetry of the magnetic equilibrium → **upshift/downshift of $k_{\parallel}$**

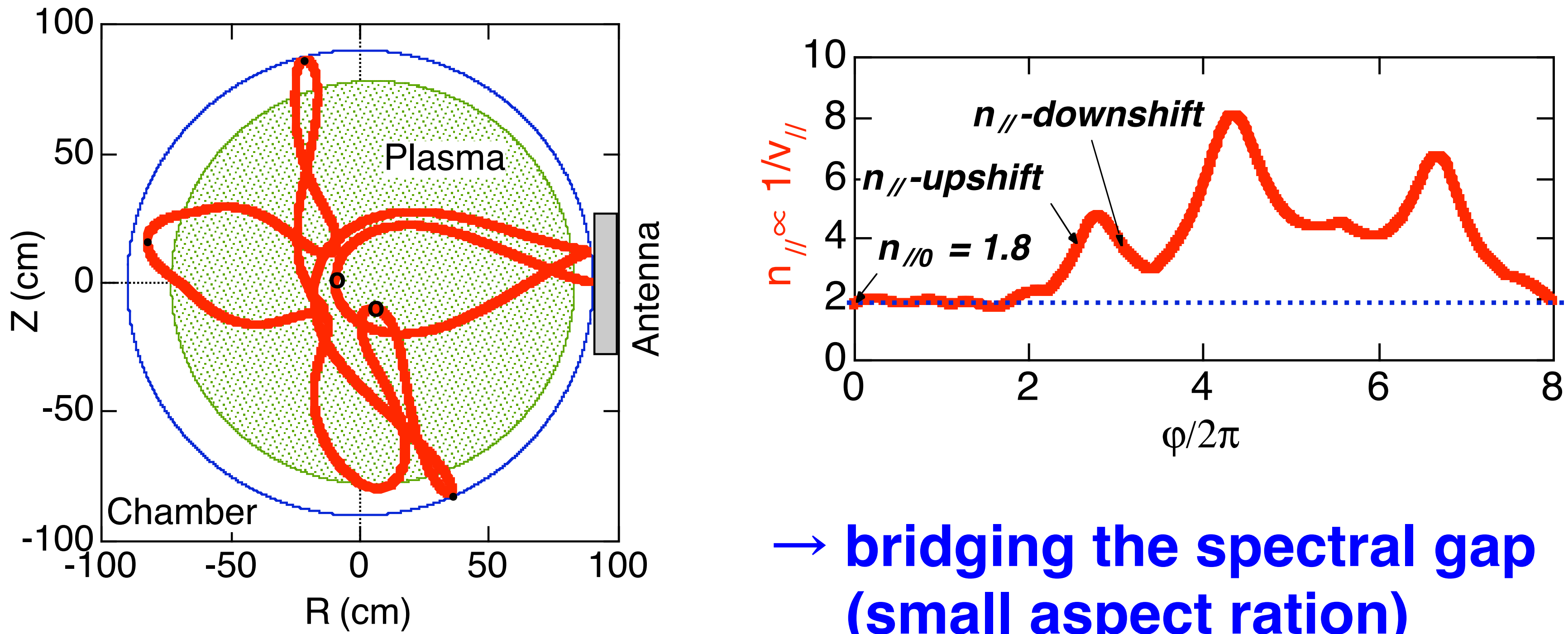

→ bridging the spectral gap (small aspect ration)

LH current drive simulations: the spectral gap problem

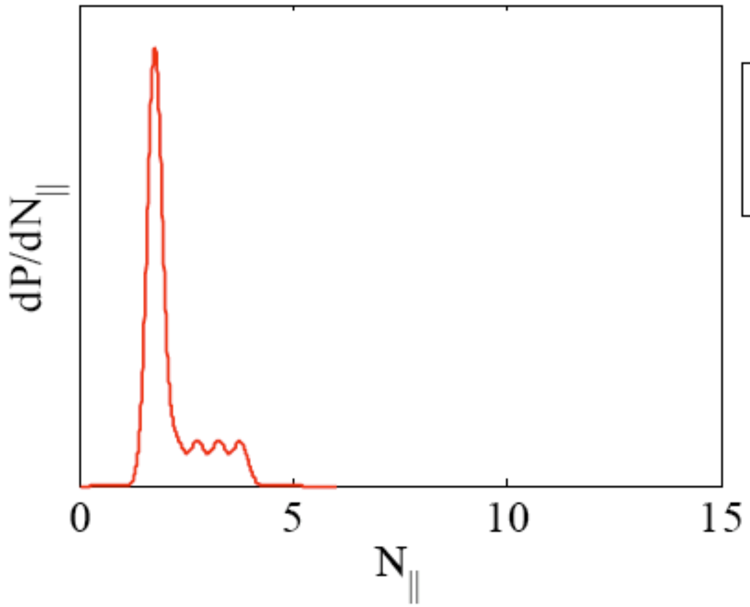

$$\frac{v_{\|res}}{c} = \frac{1}{N_{\|}}$$

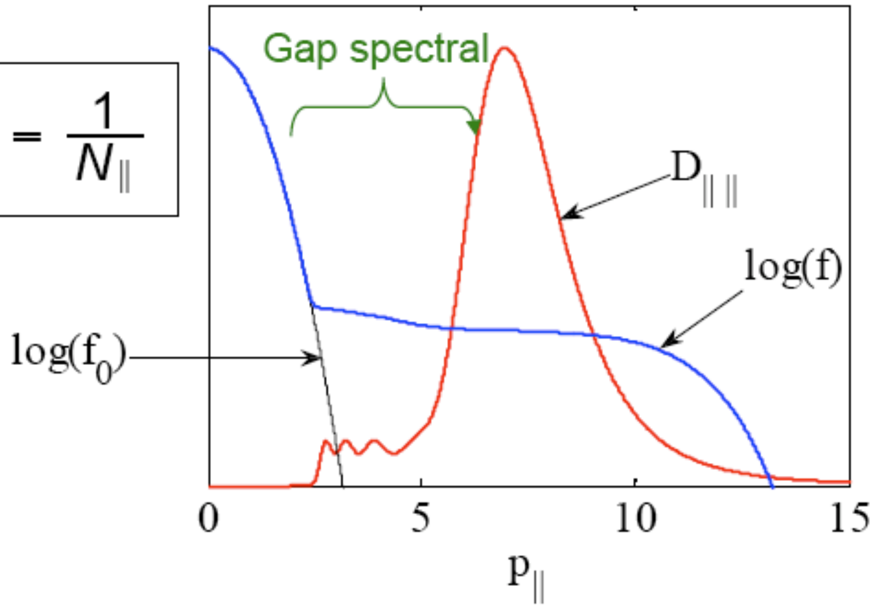

The **spectral gap** is bridged by a small fraction of the LH power at high $n_{||}$ which pulls out a tail of fast electrons from the bulk which itself contributes to absorb the remaining part of the power at low $n_{||}$

J. Decker, and Y. Peysson, in Proc. 33rd EPS Conf. on Plasma Phys. and Contr. Fusion, 2006.

In concentric magnetic configuration (cylindric or toric) , the domain of propagation of the LH wave is bounded by cut-off, accessibility, **caustics where k_ρ=0**, and possibly Landau damping (absorption).

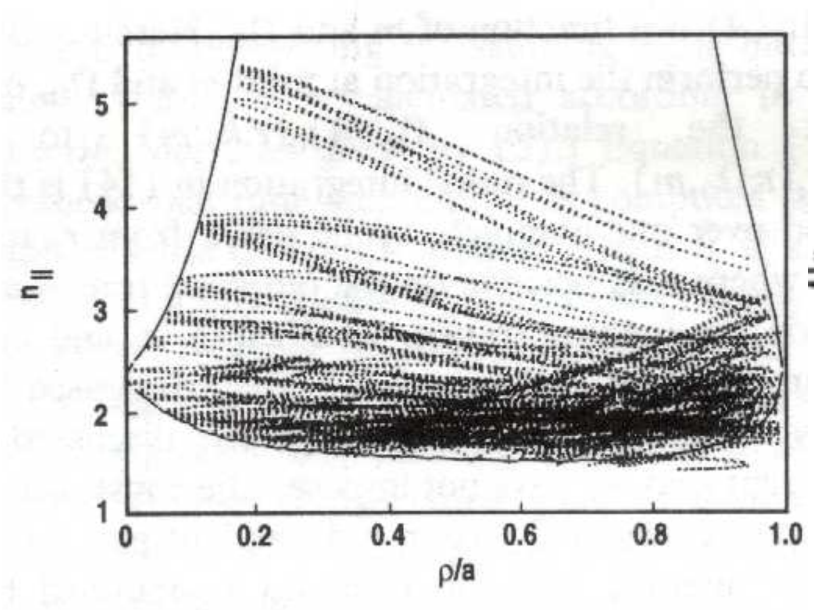

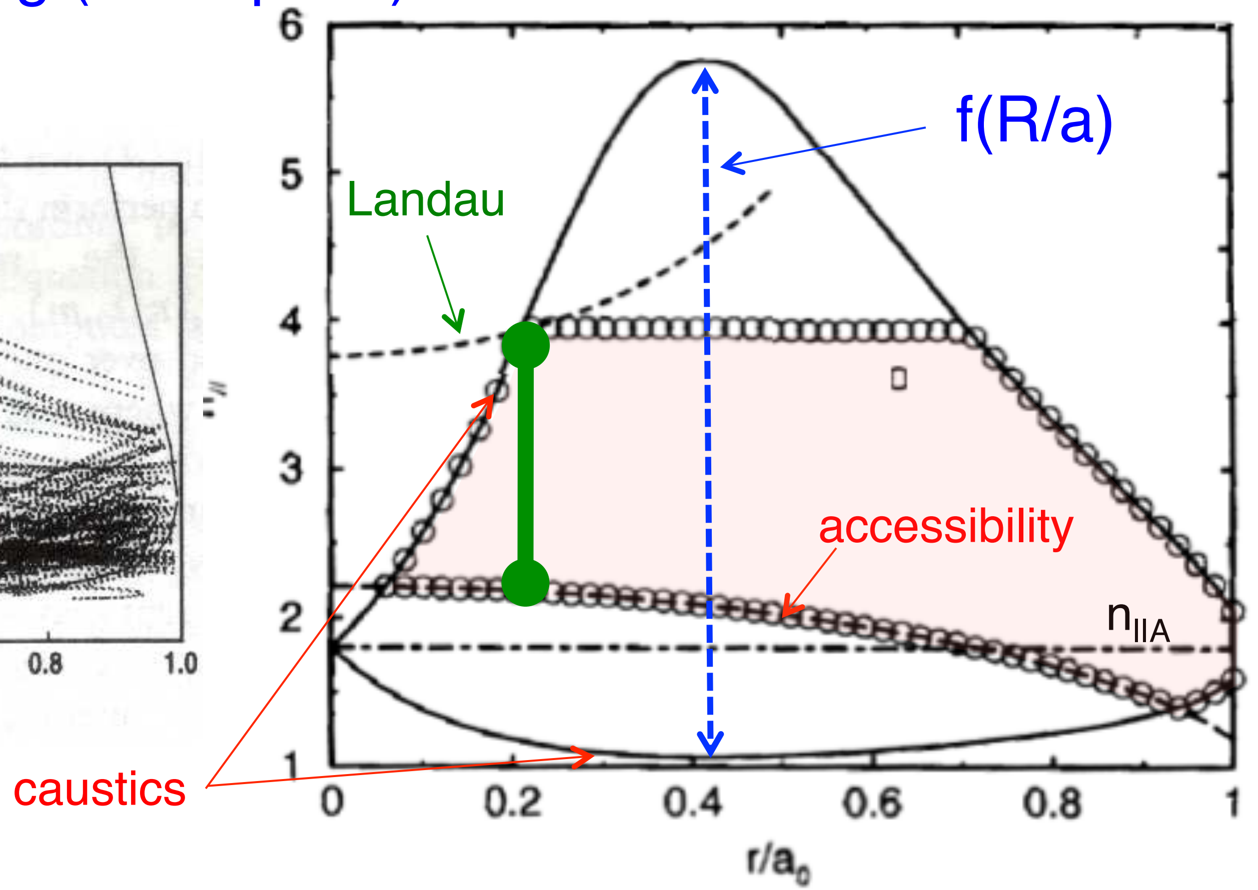

Link between ray tracing and Fokker-Planck codes

- The RF wave is described by a set of rays
- The plasma is divided into incremental flux surfaces
- D_{ql} is calculated on each flux surface (plane wave model):
    - contribution of all rays
    - contribution of all passes of the same ray

$$\mathbf{D}_{QL}(\psi,\vec{p}) = \sum_{y} \mathbf{D}^{y}_{QL}(P_y,\psi,\vec{p})$$

Ray power flow equation

$$\frac{dP_y(\psi)}{dV(\psi)} = P_y^{abs}(\psi)$$

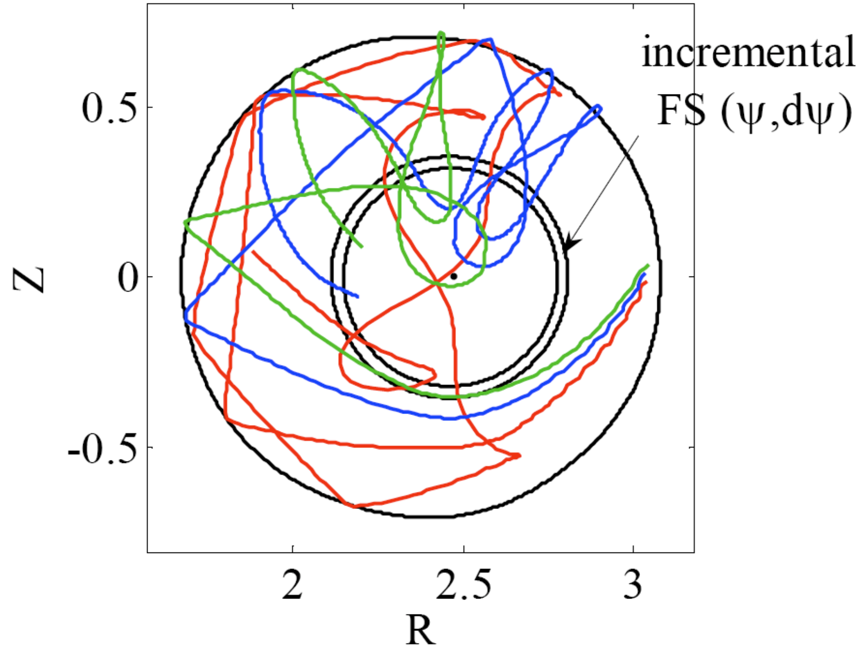

J. Decker, and Y. Peysson, in Proc. 33rd EPS Conf. on Plasma Phys. and Contr. Fusion, 2006.

Self-consistent quasilinear calculations

$$P_{y,\mathrm{lin}}^{\mathrm{abs}}(\psi)$$

linear absorption

ray power

$$\frac{dP_y(\psi)}{dV(\psi)} = P_y^{\mathrm{abs}}(\psi)$$

QL diffusion coefficient

$$\mathbf{D}_{\mathrm{QL}}(\psi,\vec{p}) = \sum_y \mathbf{D}_{\mathrm{QL}}^y(P_y,\psi,\vec{p})$$

Fokker-Planck equation

$$C(f) + \frac{\partial}{\partial\vec{p}}\left[\mathbf{D}_{\mathrm{QL}}\frac{\partial f}{\partial\vec{p}}\right] + T(f) = 0$$

$$J(\psi)$$

QL absorption

$$P_y^{\mathrm{abs}}(\psi) = \int \varepsilon(p)\frac{\partial}{\partial\vec{p}}\left[\mathbf{D}_{\mathrm{QL}}^y\frac{\partial f}{\partial\vec{p}}\right] d^3p$$

J. Decker, and Y. Peysson, in Proc. 33rd EPS Conf. on Plasma Phys. and Contr. Fusion, 2006.

Bounce-averaged electron momentum distribution function

LUKE

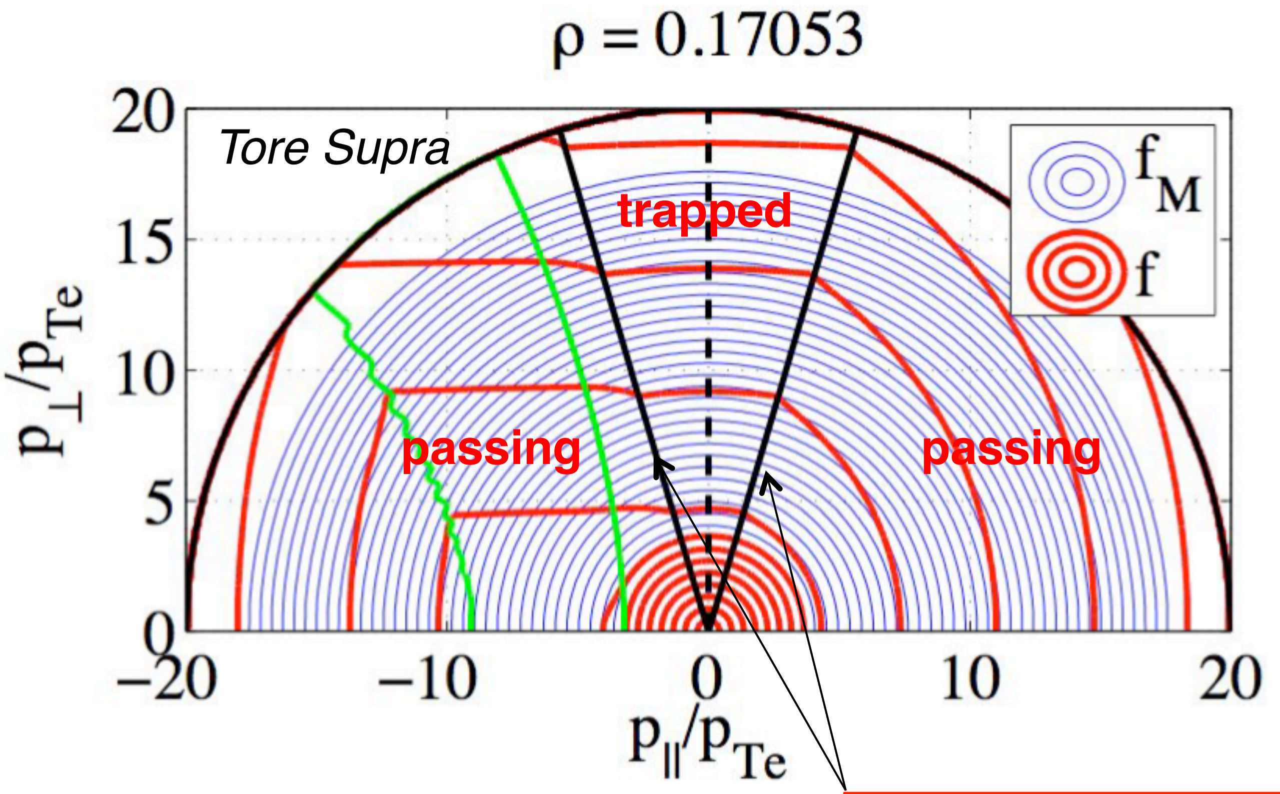

$$\xi_{0T} = \sqrt{1 - \frac{B_{\min}(\psi)}{B_{\max}(\psi)}}$$

Momentum space dynamics on the magnetic flux surface ψ

J. Decker and Y. Peysson, Euratom-CEA, 2004, report, EUR-CEA-FC-1736

C3PO

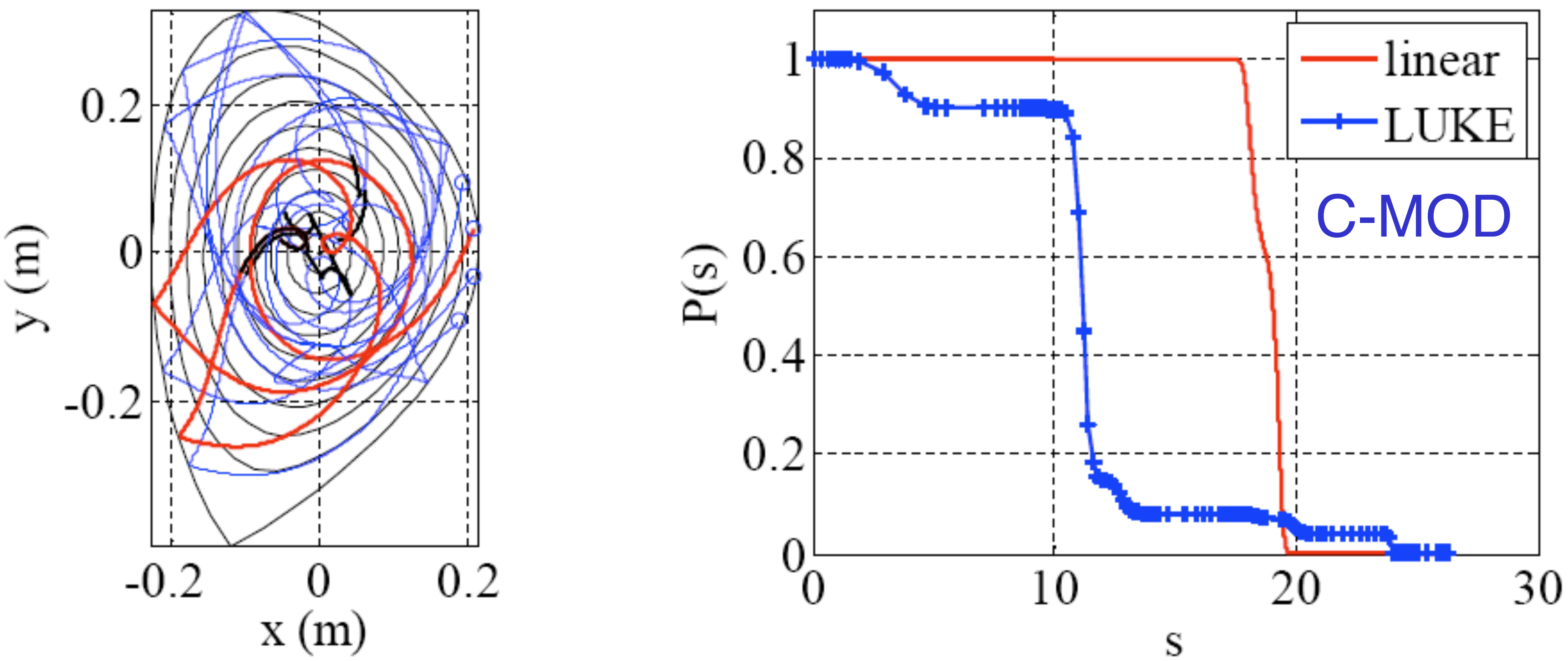

Very important quasilinear ray inter- and intra-coupling

Y. Peysson and J. Decker, Theory of fusion plasmas, 2008, 1069, AIP, 176-187

Lower Hybrid current drive in Tore Supra: strong absorption regime (single pass)

FAM antenna

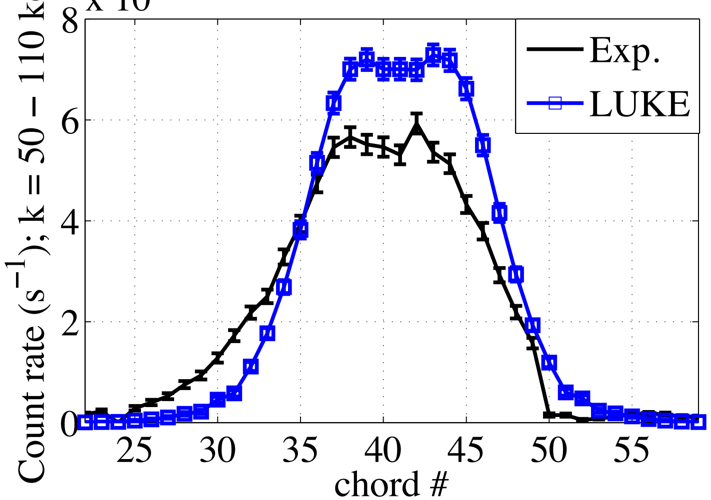

PAM antenna

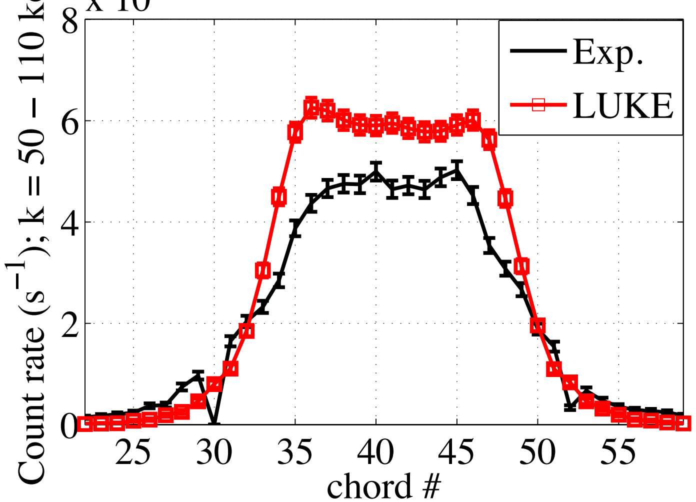

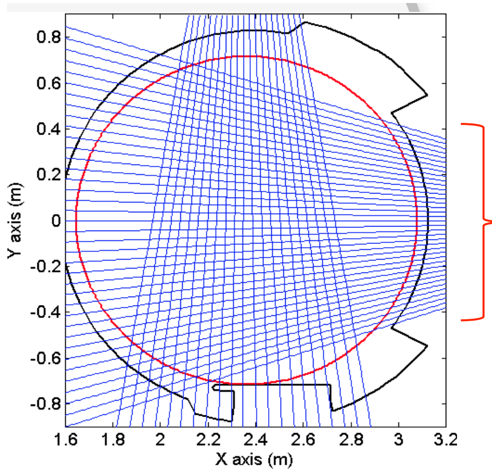

Fast electron bremsstrahlung

Y. Peysson and F. Imbeaux, Rev. Sci. Instr., 1999, 70, 10, pp. 3987-4007

E. Nilsson, J. Decker, et al. EPS conf. (2012)

Lower Hybrid current drive in Tore Supra: weak absorption regime (multiple pass)

Tore Supra #32299

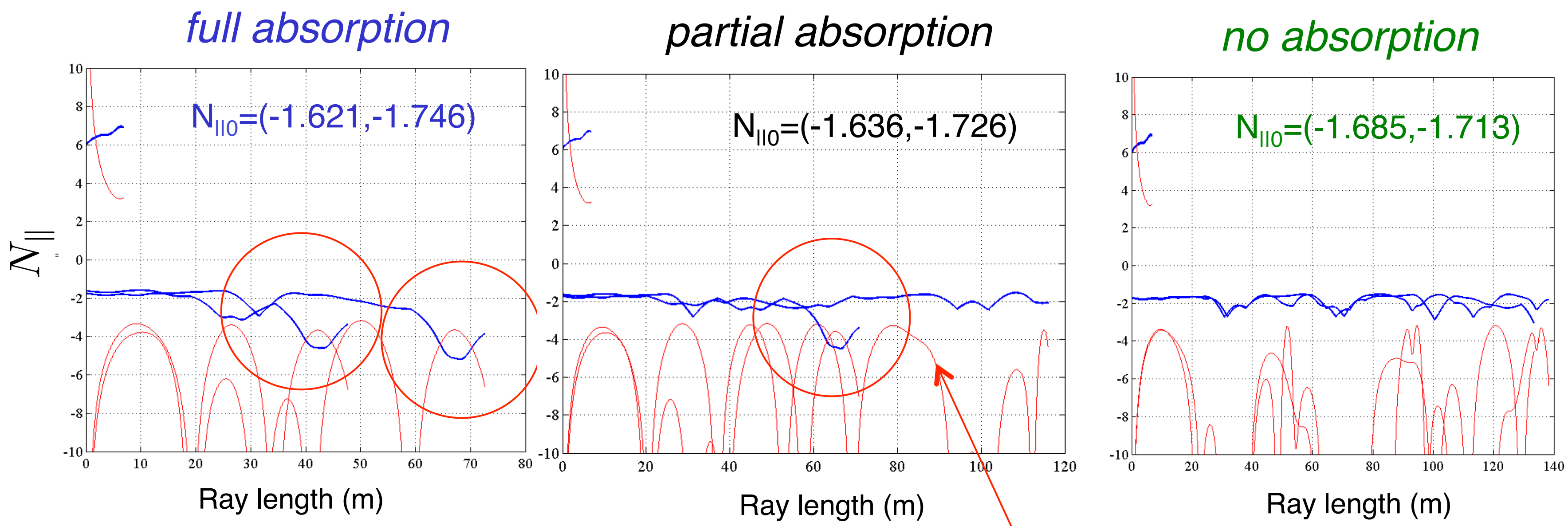

$$\frac{6.5}{\sqrt{T_e}} \propto v_\phi = 3 - 4 \times v_{th}$$

Lack of robustness of LH current drive simulations in the multipass absorption regime (most present day tokamaks) when the spectral gap is bridged by toroidal $N_{\parallel}$ upshift → Simulations often done well beyond code validity: *ray stochasticity develops before power absorption.*

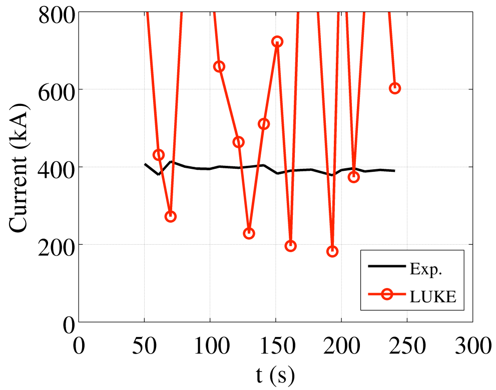

Y. Peysson, J. Decker, et al. PPCF, 53 (2011) 124028)

From ray tracing to full-wave description

rf wave ordering and code complexity

$$(\boxed{\lambda}, \boxed{\phi_B}, \boxed{R})$$

wave length | beam width | gradients length

Increasing level of complexity

$$\lambda \ll \phi_B \ll R \Rightarrow \text{ray-tracing}$$

$$\lambda \sim \phi_B \ll R \Rightarrow \text{beam-tracing}$$

$$\lambda \ll \phi_B \sim R \Rightarrow \text{WKB full-wave}$$

$$\lambda \sim \phi_B \sim R \Rightarrow \text{full-wave}$$

Y. Peysson and J. Decker, Theory of fusion plasmas, 2008, 1069, AIP, 176-187

Full-wave approach

- Full-wave description allows to describe LH wave characteristics from **propagative** (strong damping, *ray equation*) to cavity (very weak damping, *normal mode master equation*) regimes.

$$\nabla \times \nabla \times \mathbf{E} = \omega^2 \varepsilon_0 \mu_0 \mathbf{E} + \mathbf{i} \omega \mu_0 \left[\mathbf{J} + \mathbf{J_A} \right]$$

- Perfectly conducting wall for boundary conditions :

$$\mathbf{n} \times \mathbf{E} = \mathbf{0}$$

No separation with absorption !

- Local dielectric properties : $\mathbf{J} = \mathbb{S}(f_0) \cdot \mathbf{E}$

- Fourier transform method (toric case: TORLH, Irzak code), real space technique (cylindrical + toric case ELECTRE, *ELECTRE-T*)

Weak variational approach

Find the stationary point of the bilinear form

$$L(\mathbf{E},\mathbf{E}^*) = \int_V dr \left[(\nabla\times\mathbf{E})\cdot(\nabla\times\mathbf{E}^*) - \frac{\omega^2}{c^2}\mathbf{E}^*\cdot\mathbb{K}\cdot\mathbf{E} - \frac{4i\pi}{c^2}\mathbf{E}^*\cdot\mathbf{J}_A \right]$$

with respect to all variations δE^*, subject to the condition $\mathbf{n}\times\delta\mathbf{E}^*|_\Sigma = 0$

on the boundary Σ (wall), with the principle condition of perfect conductive wall.

Trial functions approximate the solution over several wavelengths: $\lambda >> \Delta_{grid} >> \nabla^{-1}$: 4 eikonal eigenfunctions for cold plasma dispersion relation. *Radial matching conditions*

$$\mathbf{E}(r,\theta,\phi) = exp(in\phi + im\theta)\sum_{l=1}^{L} H_l(r)\,\Sigma_{i=1}^{4}\alpha_{i,l}\mathbf{E}_{i,l}r^{\lambda_{i,l}}$$

Polarization

Eigenvalues

D. Moreau, Y. Peysson, et al., Nucl. Fusion, 1990, 30, 97

Cylindrical full-wave LH calculations

LH wave accessibility

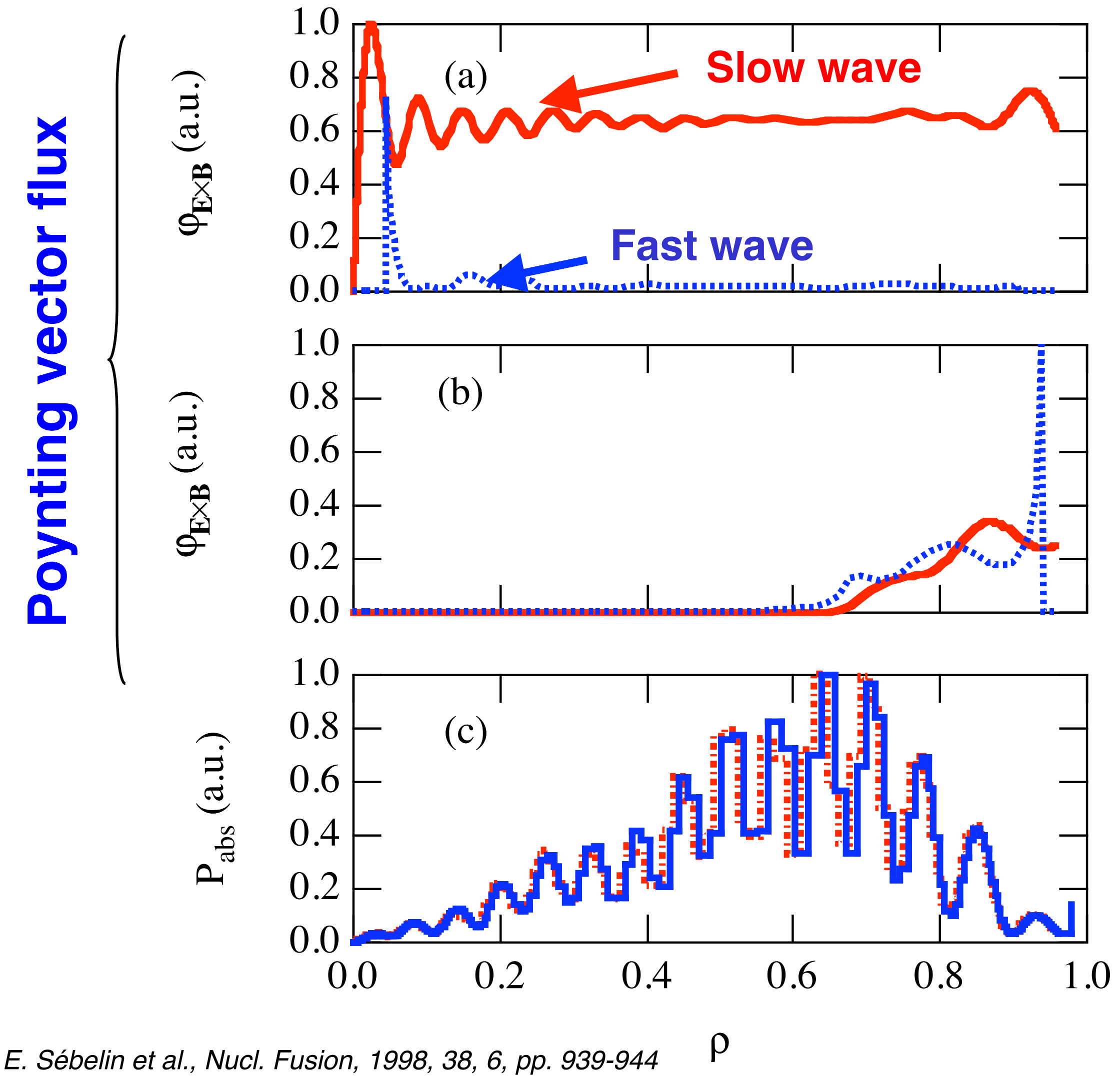

$n_{||} = 1.4$ ($> n_{||a} = 1.35$)

$n_{||} = 1.3$ ($< n_{||a} = 1.35$)

ELECTRE

Y. Peysson, E. Sébelin et al., Nucl. Fusion, 1998, 38, 6, pp. 939-944

Cylindrical ray tracing LH calculations

LH wave accessibility

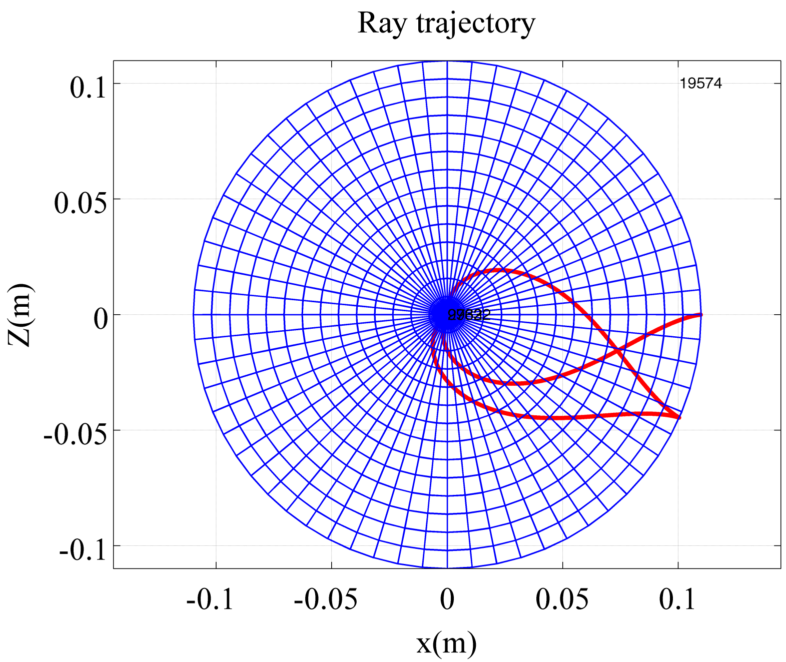

$n_{\parallel} = 1.4$ ($> n_{\parallel a} = 1.35$)

Slow wave

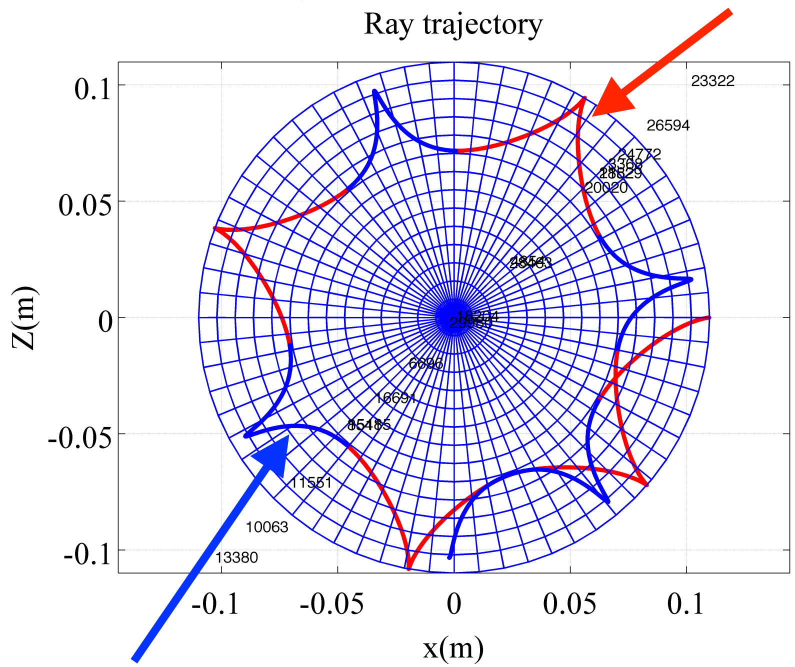

Fast wave

$n_{\parallel} = 1.3$ ($< n_{\parallel a} = 1.35$)

Y. Peysson et al., 2012 Plasma Phys. Control. Fusion 54 045003

Y. Peysson, E. Sébelin et al., Nucl. Fusion, 1998, 38, 6, pp. 939-944

C3PO

Toroidal full-wave LH calculations (Fourier decomposition)

TORLH

$N_m \geq 1000$
$N_r \geq 500$
$N_\phi \geq 500$

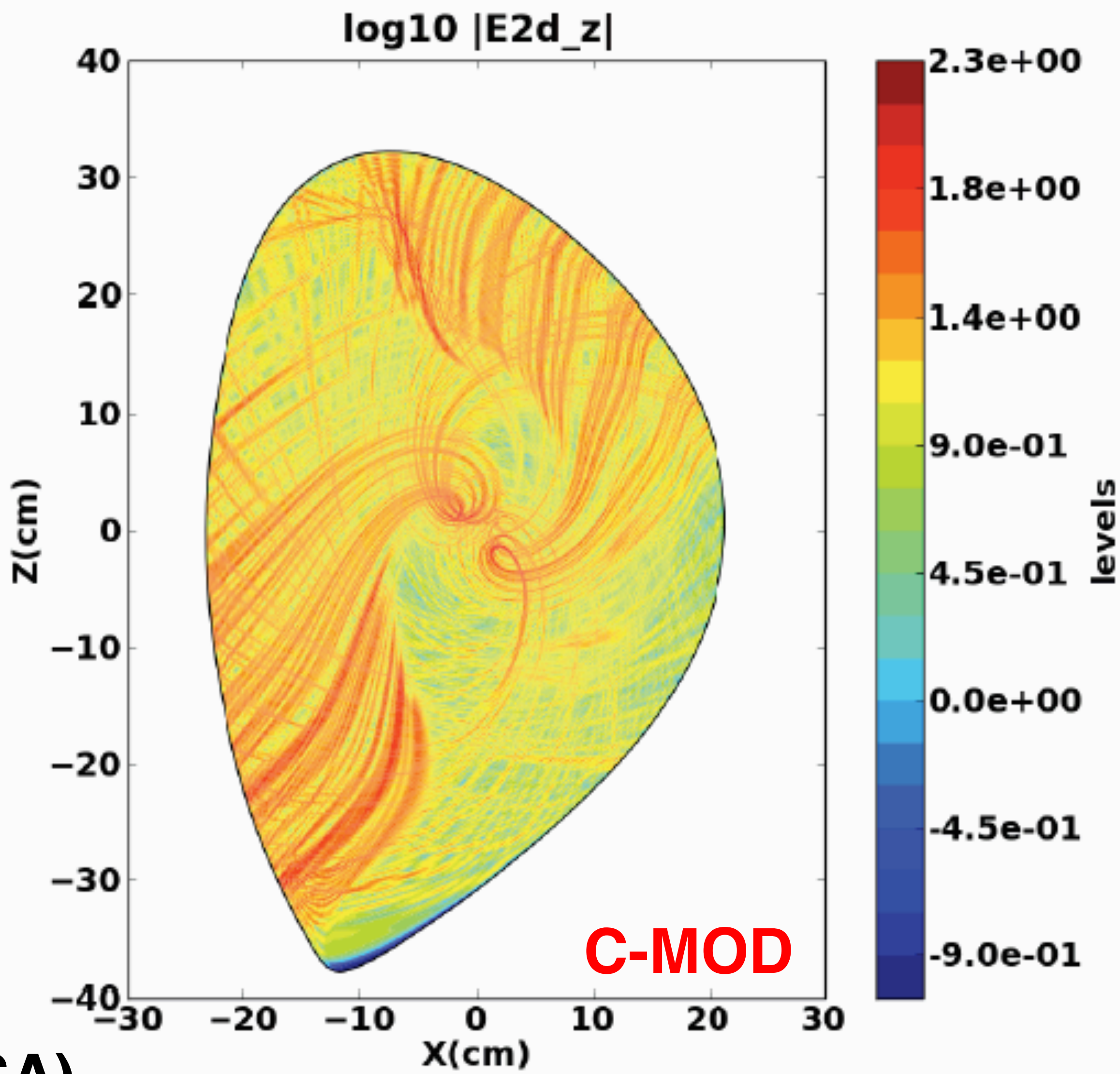

(PSFC/MIT, USA)

J. C. Wright, P. T. Bonoli, et al., Phys. Plasmas, 2004, 11, pp. 2473-2479

Toroidal full-wave LH calculations (Fourier decomposition)

Rescaling technique to avoid an excessive numerical effort (LH physics ?)

GLOBUS-M tokamak: R_0 = 36 cm, a_0 = 24 cm, $n_{e0} = 4\times10^{19}\ m^{-3}$, B_{tor} = 0.5 T, I_p = 500 kA, f = 2.45 GHz.

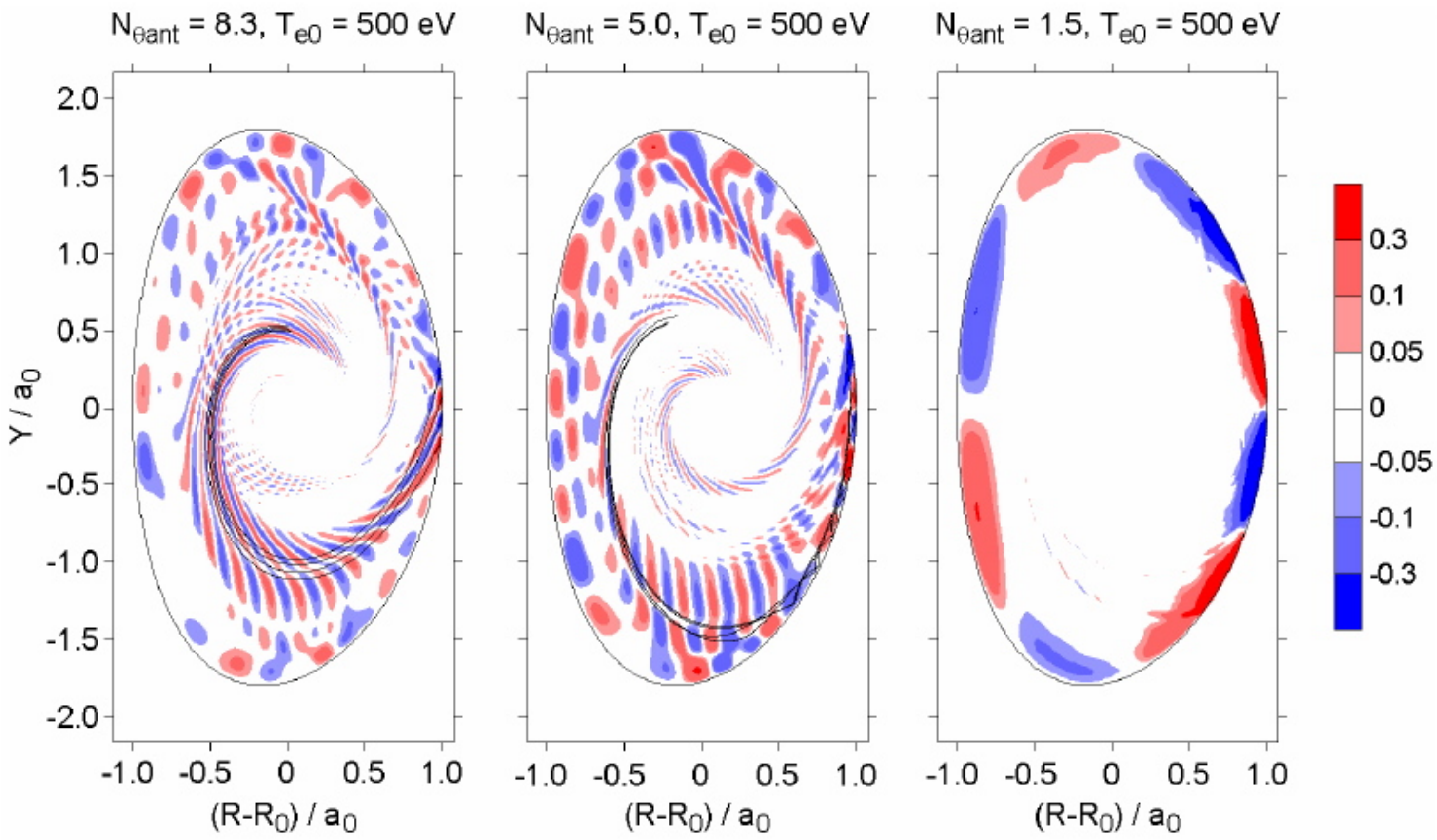

Parallel component of the electric field $E_{\parallel}$ (in a.u.).

Irzak code

(Ioffe Institute,RF)

Toroidal full-wave in real space

Extrapolation of concepts used in cylindrical geometry may not be extrapolated to the toroidal configuration: *impossible to find matching conditions in both radial and poloidal direction*

Need a standard approach (discretization less than the wave-length) but incorporating parallel processing in the numerical approach from the initial design (domain decomposition, mixed-augmented formulation). Keep the resolution in real space though $k_{||}$ may be difficult to calculate for the link with the Fokker-Planck code. *Code may be used locally for other types of waves*

Time-harmonic Maxwell wave equation

$$\begin{aligned} \mathrm{curl}_\nu \mathrm{curl}_\nu \boldsymbol{u}_\nu - k^2 \underline{\boldsymbol{\epsilon}} \boldsymbol{u}_\nu &= \boldsymbol{f}_\nu \quad \text{in } \widetilde{\Omega}, & (1) \\ \mathrm{div}_\nu (\underline{\boldsymbol{\epsilon}} \boldsymbol{u}_\nu) &= g_\nu \quad \text{in } \widetilde{\Omega}, & (2) \\ \boldsymbol{u}_\nu \times \boldsymbol{n} &= \boldsymbol{h}_\nu \quad \text{on } \widetilde{\Gamma} := \partial\widetilde{\Omega}, & (3) \end{aligned}$$

in a bounded domain $\widetilde{\Omega} \subset \{(R, Z) \in \mathbb{R}^2 \,|\, R > 0\}$, with $\nu \in \mathbb{Z}$. This problem arises from the 3D Maxwell wave equation – given in the torus $\Omega := \widetilde{\Omega} \times [0, 2\pi)$ – after Fourier decomposition of the solution $\boldsymbol{u}$:

$$\boldsymbol{u}(R, Z, \phi) = \sum_{\nu \in \mathbb{Z}} \boldsymbol{u}_\nu (R, Z) e^{\iota \nu \phi} \tag{4}$$

Relations between cartesian and toroidal coordinates:

$$x = R\cos\phi, \quad y = R\sin\phi, \quad z = -Z. \tag{5}$$

Y. Peysson, J. R. Roche, et al., RF Top. Conf. (2009)

Time-harmonic Maxwell wave equation

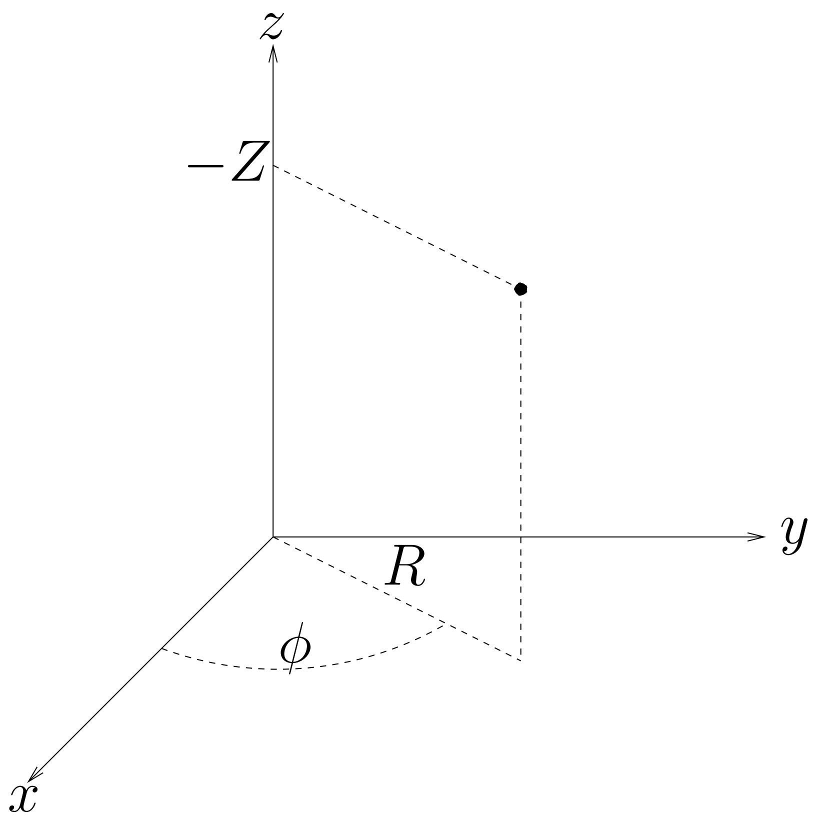

C. Kirsch, Private comm. 2007

For vector fields $\boldsymbol{F} = \boldsymbol{F}(R, Z)$:

$$\mathrm{curl}_\nu \boldsymbol{F} := \mathrm{curl}\boldsymbol{F} + \frac{\iota\nu}{R}\boldsymbol{e}_\phi \times \boldsymbol{F} \quad (6)$$

$$\mathrm{div}_\nu \boldsymbol{F} := \mathrm{div}\boldsymbol{F} + \frac{\iota\nu}{R}\boldsymbol{e}_\phi \cdot \boldsymbol{F} \quad (7)$$

- dualization of divergence and boundary conditions (2), (3) $\rightsquigarrow$ Lagrange multipliers $p, \boldsymbol{\lambda}$
- discretization with modified Taylor-Hood elements: curl-div-conforming nodal elements, as opposed to curl-conforming edge elements

Matlab test code

Conclusions and prospects

Conclusions and prospects

- The Lower Hybrid is still nowadays the most efficient experimentally proven non-inductive current drive method, but likely the one for which the physical mechanismes are the less well understood, despite large experimental an numerical efforts. Poor intepretation and extrapolation capabilities…

- Realistic simulations are routinely based on coupled ray tracing and Fokker-Planck calculations (magnetic equilibrium + energy transport self-consistency). Reasonable agreement with experiments in strong absorption regime, but very poor in weak one (the most frequent), because of the stochastic behaviour of ray propagation. Solution highly sensitive to any perturbation

- The progresses in computer technology have allowed to perform full-wave calculations in toroidal geometry, all based on a Fourier mode description (very large numerical effort). There are large differences in the current density profile prediction between full-wave and ray tracing (linear absorption, no magnetic equilibrium consistency)

- An cylindrical full-wave in real space have been developped based on an original approach with eikonal eigenfunctions for trial functions. Not extrapolable to the toroidal case. But the real space full-wave remains an attractive option to validate the Fourier approach

- Theoretical developments and numerical tests to validate principles have been carried out in the past years. The full toroidal full-wave code remains to be done !